X-ray & radio observations of type II Plateau SNe & Equipartition Factors

Alak Ray

Tata Institute of Fundamental Research, Mumbai, India

with Naveen Yadav, Sayan Chakraborti, Randall Smith, Keiichi Maeda (Kyoto Univ!) et al

Submitted 2013, N. Yadav et al
+ 2013, 2012 ApJ, S. Chakraborti et al

Ongoing Program to observe type II Plateau type SN

with Chandra and EVLA & GMRT that probes X-ray and radio bands (high and low frequencies) to detect the nature of thermal and non thermal radiation from SNIIP

Examples: SN 2004dj, SN 2011ja, SN 2012aw, SN 2013ej

Images courtesy of:
Chandra X-ray Observatory; NRAO/AUI & GMRT/NCRA-TIFR

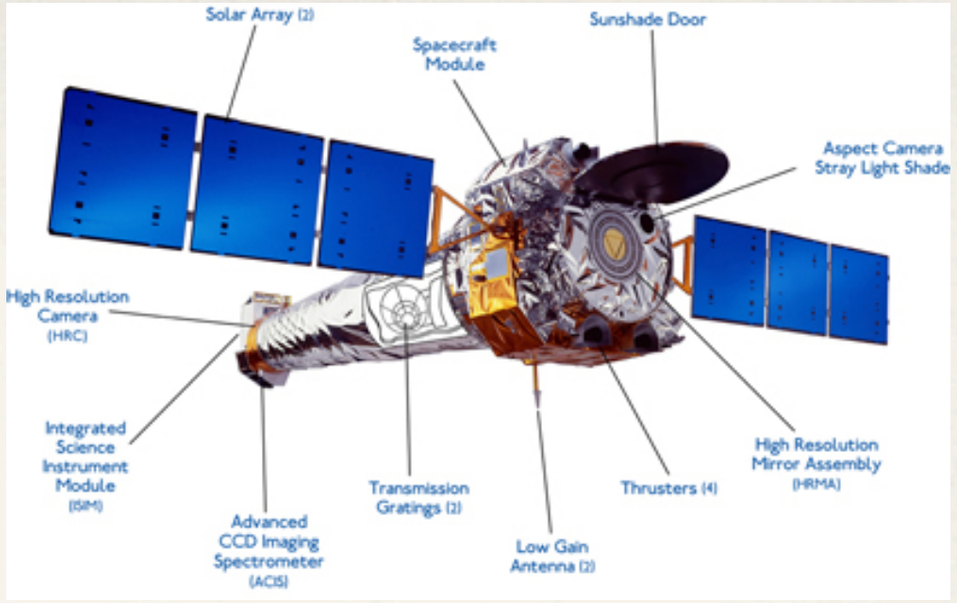

Radio and X-ray near contemporaneous observations

- Can constrain equipartition factors ε_B & ε_e within a narrow range.
- If X-ray bright objects (e.g. SN 2004dj) can be detected and followed, we may quantify the Inverse Compton (IC) vs thermal emission mechanisms
- If IC is detected then $\varepsilon_e \gamma_{min}$ are determined by comparing X-ray and OIR luminosities
- Since IC requires γ_{min} ~ 30-100, for X-ray band this allows the determination of ε_e.
- For thermal X-ray emission, X-ray observations can constrain mass loss rate in wind set up by the progenitor star.
- From the mass loss rate, with the help of model evolution of stars, can constrain the progenitor star mass main seq.

How are Supernovae distributed among different types?

Nathan Smith et al, MNRAS 2011

- Volume limited sample of 80 Core Collapse Supernovae up to 60 Mpc discovered and followed up by the UC Berkeley group.

Table 1. Volume-limited core-collapse SN fractions

SN Type	fraction	error
	(%)	(%)
Ic	14.9	+4.2/−3.8
Ib	7.1	+3.1/−2.6
Ibc-pec	4.0	+2.0/−2.4
IIb	10.6	+3.6/−3.1
IIn	8.8	+3.3/−2.9
II-L	6.4	+2.9/−2.5
II-P	48.2	+5.7/−5.6
Ibc (all)	26.0	+5.1/−4.8
Ibc+IIb	36.5	+5.5/−5.4

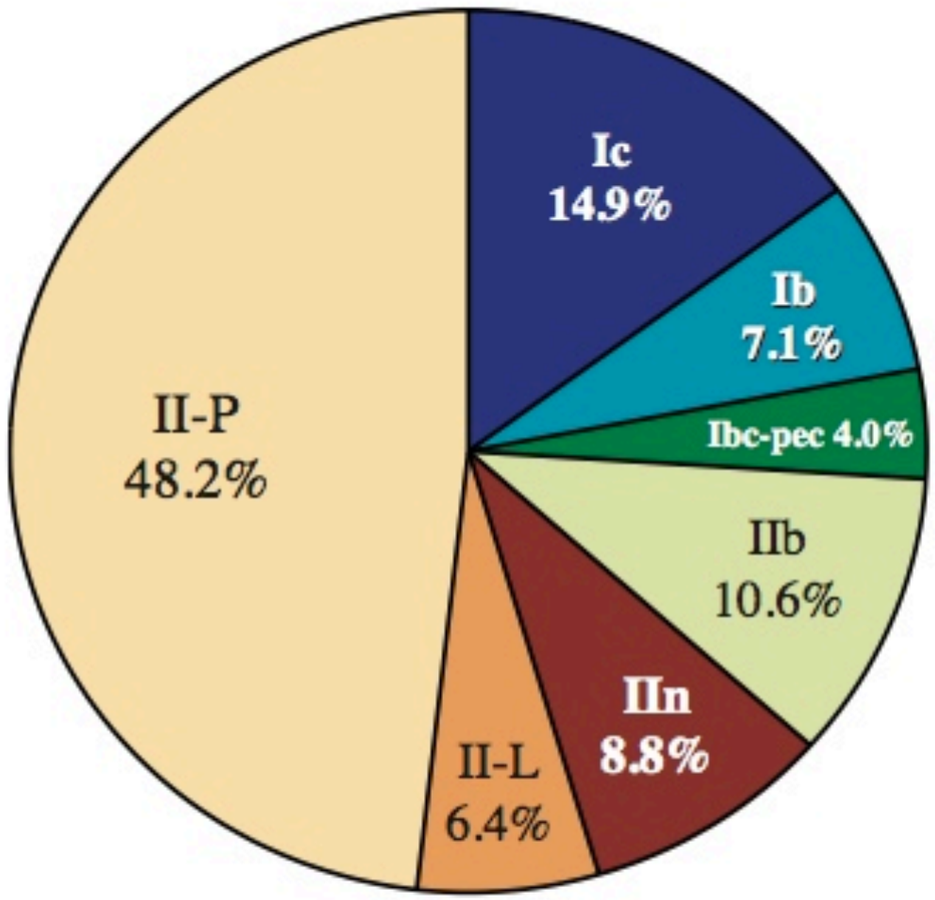

Core-Collapse SN Fractions

Sampling the IMF consistently w. observed fractions of CCSN types

- Higher initial mass leads to higher mass loss rates in a single star evolution, and a greater stripping of the H & He envelopes.

- In close binary evolution & Roche Lobe overflow leads to loss of H-envelope.

- The fraction of all massive stars that lose their H envelopes as type Ibc (26%) and and with IIBs the total fraction is 36.5%

- Roughly half of SN Ic (8.8% of all CCSNe to match the fraction of SN IIn) away from the RLOF population and mixed them with single star population. SN Ic that arise from single stars are below the dashed line.

- Half of all single stars above ~ 23 Msun are able to shed their H-envelopes via winds or eruptions while the other half retain their H-envelopes until just before core collapse producing SNe IIn.

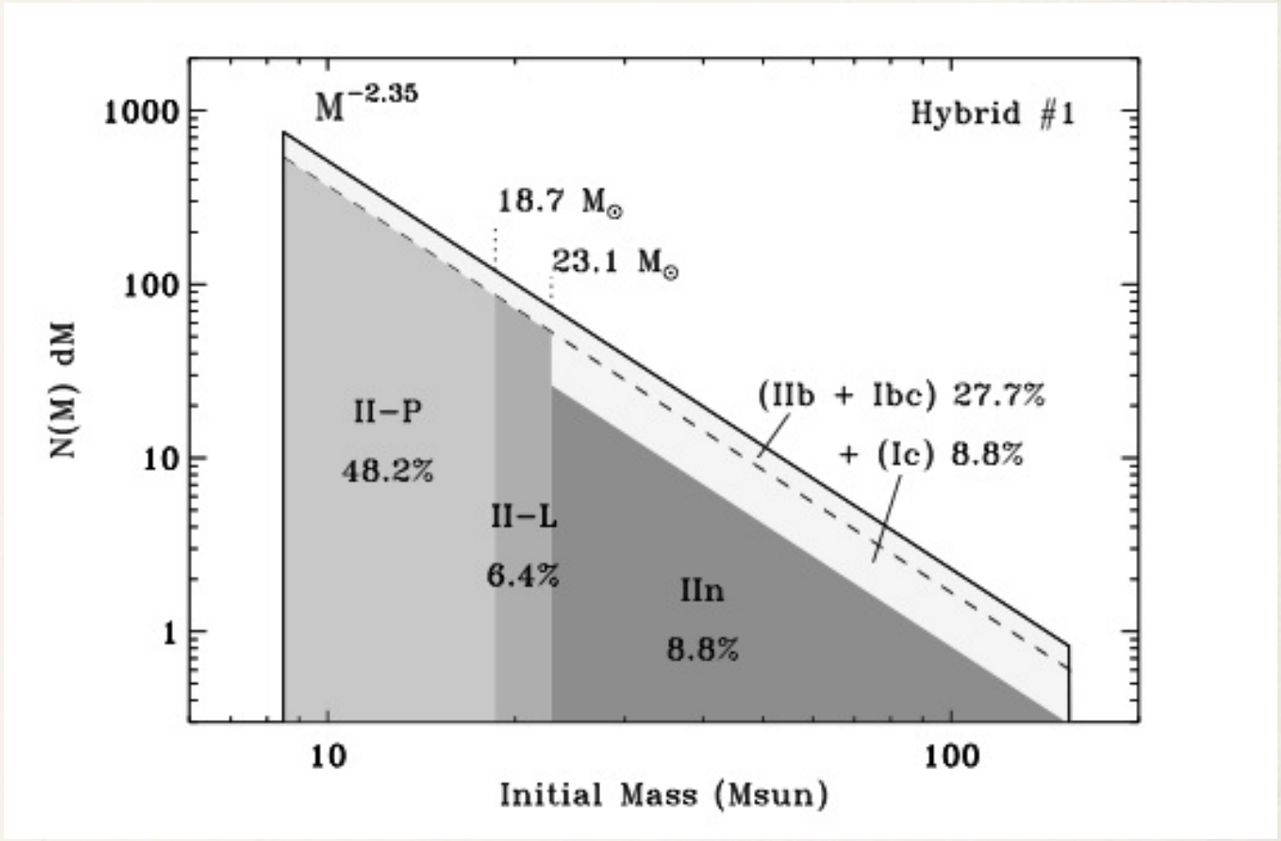

Fig 7 from: Nathan Smith et al, MN 2011: one example

A red supergiant problem?

- Type IIP progenitors were red supergiants (RSG) when they exploded
- There are massive RSG stars (M > 17 Msun) seen in the Local Group of galaxies (MW, LMC..).
- But no high mass RSG progenitors above about 17 Msun (& < 25 M for W-R star progenitors) have been found for IIP SNe.
- Smartt et al (2009) used a volume limited search for SN progenitor stars in direct detection efforts.
- RSG "Problem" may indicate: more massive stars could have high core masses to form black holes instead of neutron stars. SNe of higher M stars too faint.
- But: Walmswell & Eldridge (2012): circumstellar dust

Ugliano, Janka, et al 2012

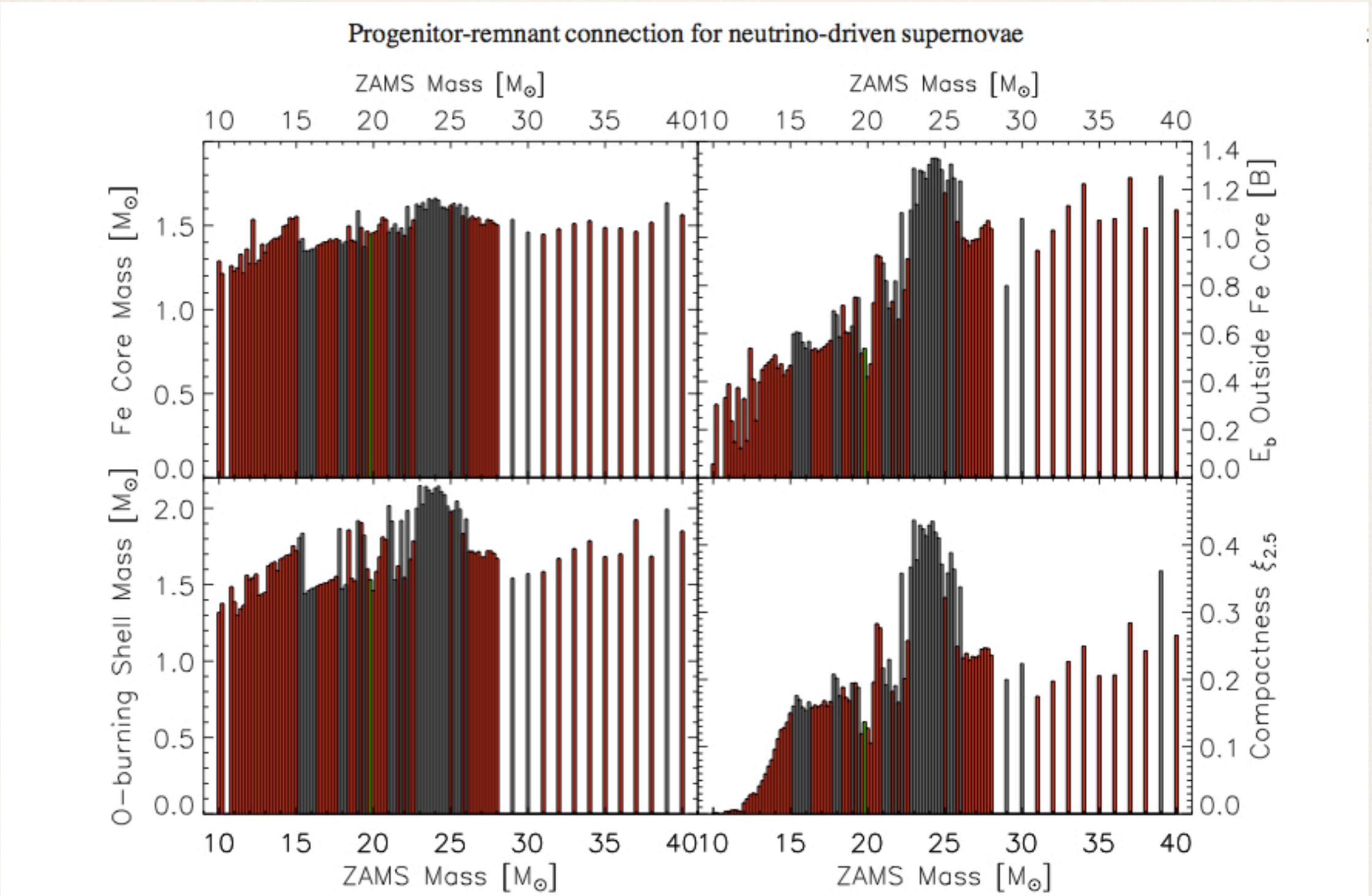

Compactness parameter $\xi_{2.5} = (M/M_{SUN})/(R(M)/1000\ km)$ has to be > 0.45
(threshold value of O'Connor & Ott 2011) for BH formation

Electron synchrotron radiation and Inverse Compton loss for e^-

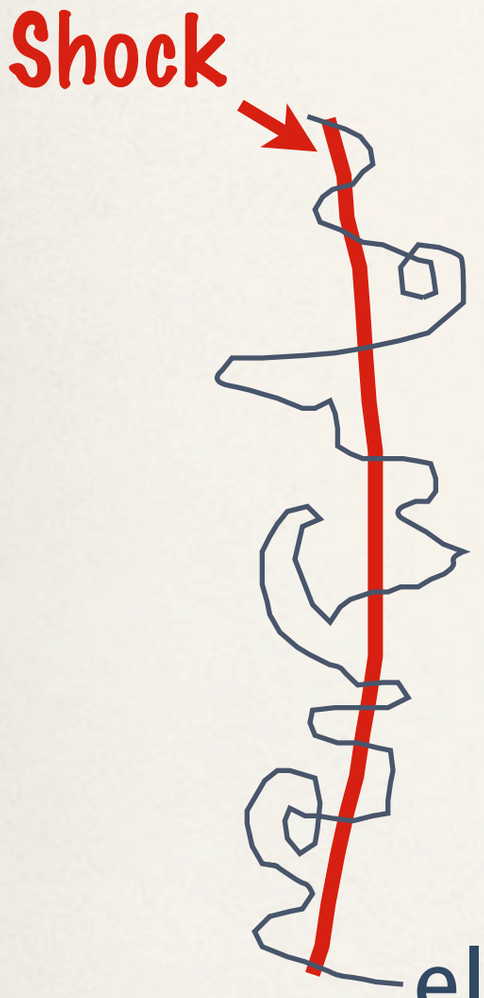

Acceleration of electrons by shock

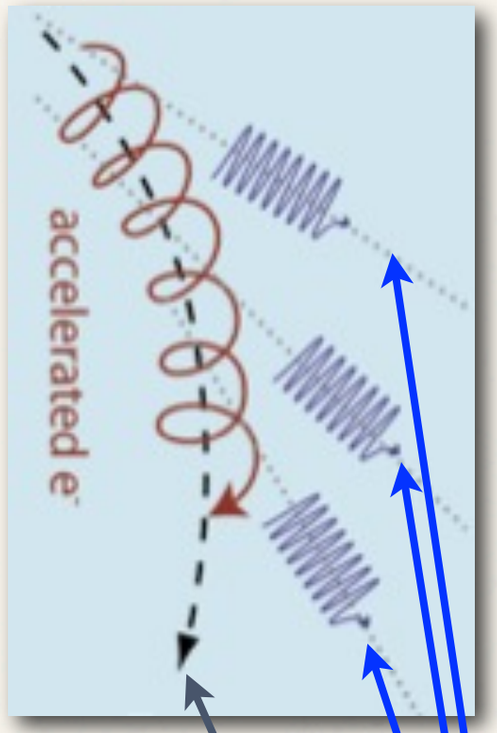

Synchrotron radiation

Inverse Compton Boosting of low energy photons

Synchrotron Emission

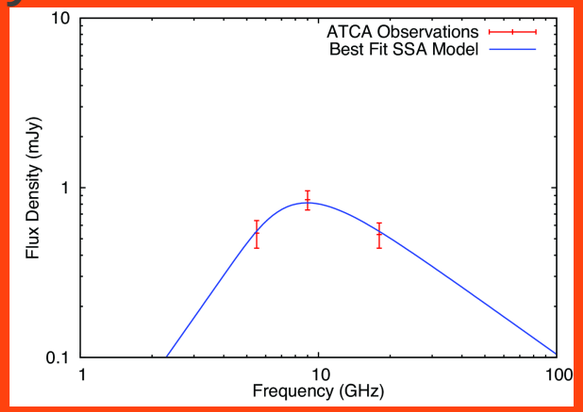

Inverse Compton

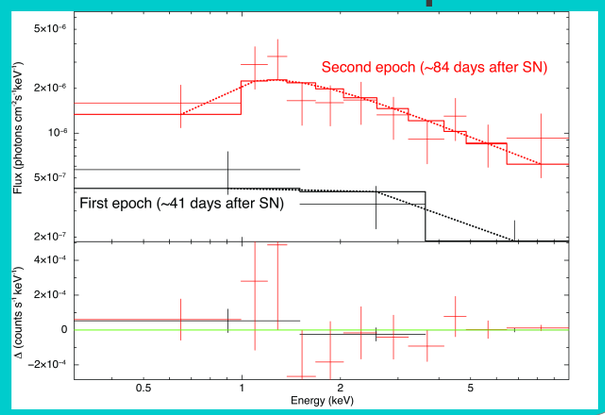

Magnetic Field Amplification

Relativistic Electron Accleration

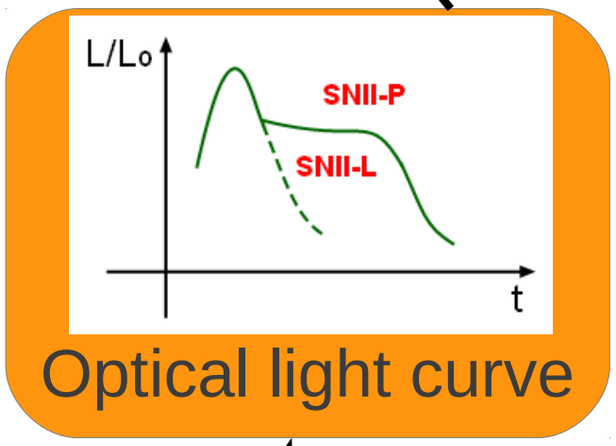

Circumstellar Interaction

Type IIP SNe

SN 2011ja
SN 2012aw

Chakraborti et al 2013 ApJ 774, 30

Yadav et al 2013 submitted

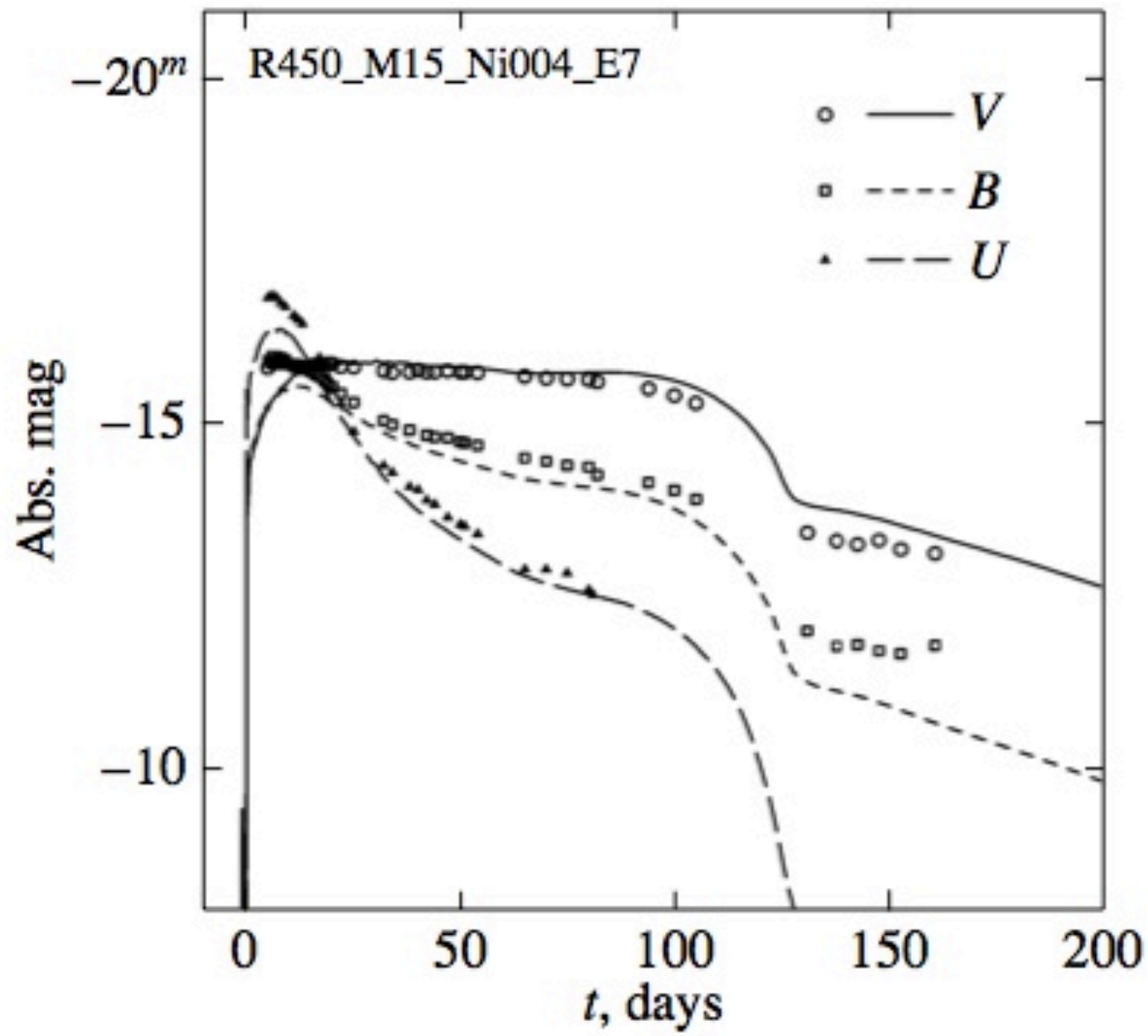

Fig. 3. U, B, V light curves of SN 1999em for model No. 1. Time from the explosion is along the horizontal axis.

"supernova impostor" SN 1954J: a highly luminous (M_V = -8.0), very massive ($M_{initial}$ > 25 Msun, eruptive star now surrounded by a dusty (A_V = 4 mag) nebula: S. van Dyk , PASP 2005.

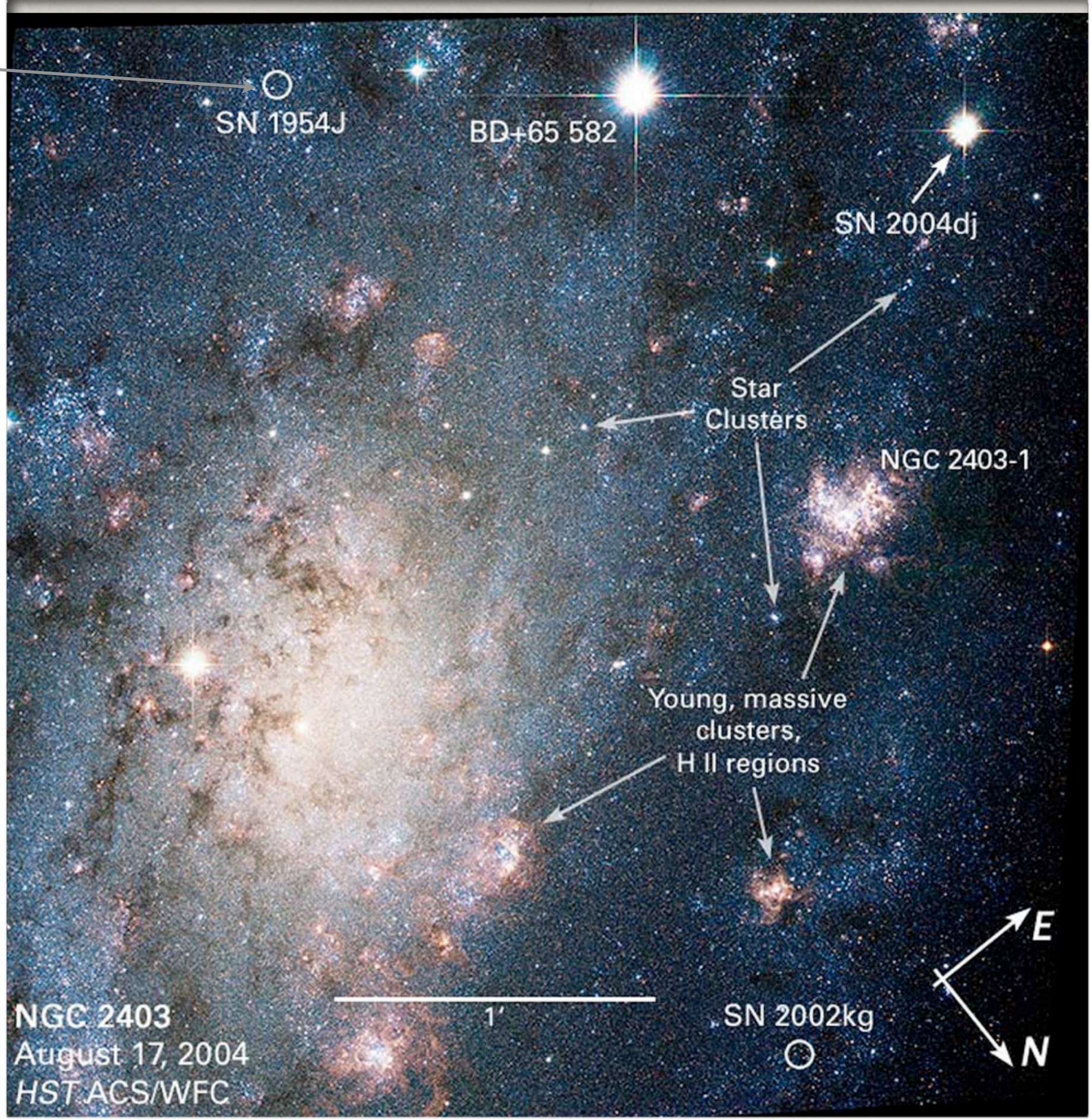

X-ray bright SN 2004dj in NGC2403

What type of stars exploded?

- Red Supergiant stars
- In recent star-forming regions of spiral galaxies
- Progenitor stars are short lived & explode from massive stars (M > 8 Msun)

SN2004dj: Chandra Observation summary

Table 1
Observation Summary of SN 2004dj with *Chandra*

Date (2004)	Exposure (ks)	Count Rate (10^{-3} s^{-1})	Flux (0.5–8 keV) (erg cm^{-2} s^{-1})
Aug 9	40.9	12.80 ± 0.56	8.81×10^{-14}
Aug 23	46.5	10.03 ± 0.47	6.98×10^{-14}
Oct 3	44.5	5.60 ± 0.36	3.30×10^{-14}
Dec 22	49.8	3.05 ± 0.25	2.02×10^{-14}

Chandra X-ray spectra of SN 2004dj

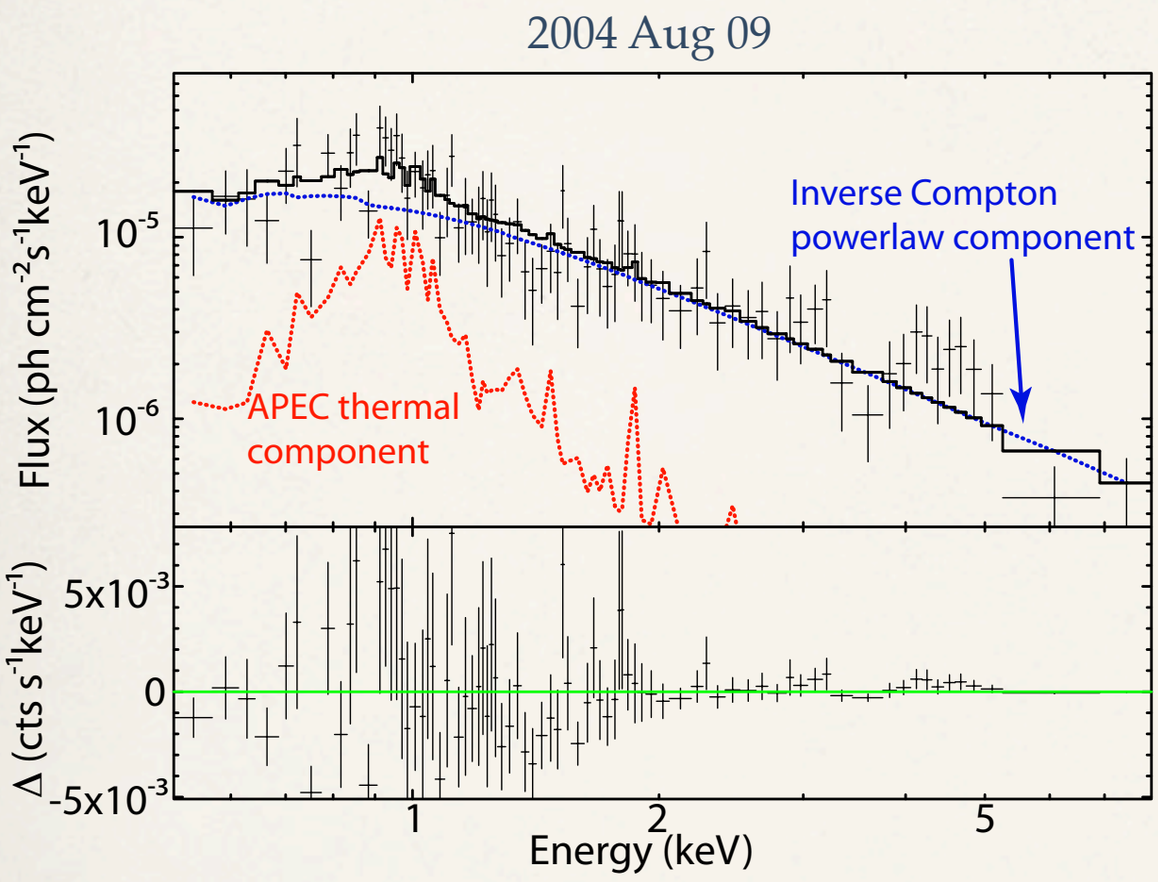

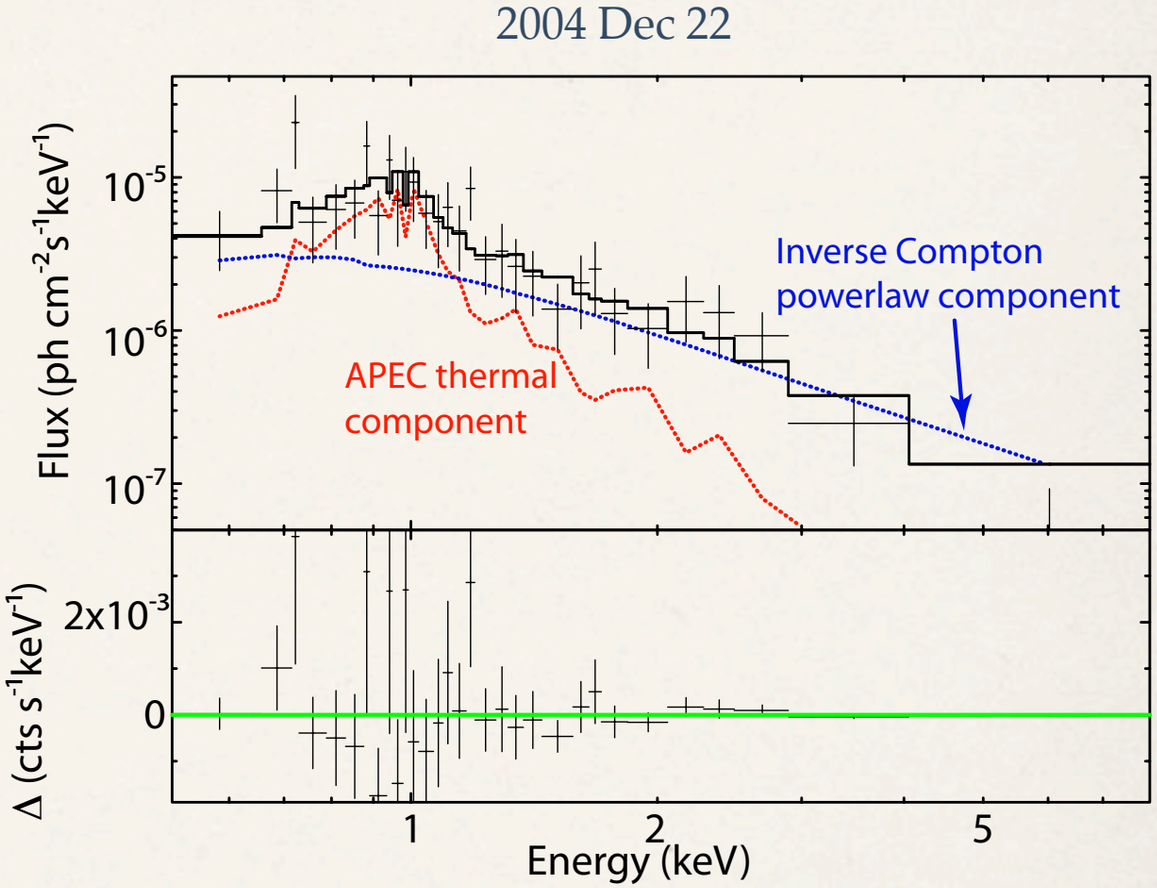

at two epochs: 1) 2004 Aug 09 and 2) 2004 Dec 22

- Extracted spectra (into XSPEC 12.7.1) jointly fitted w. power law & thermal APEC models (Randall Smith et al 2011) with photoelectric absorbing column.

Date: SN Discovered 31.76 July 2004 (UT) : This Could Be 50 +/- 21 Days After Core Collapse

Time evolution of IC & Thermal components

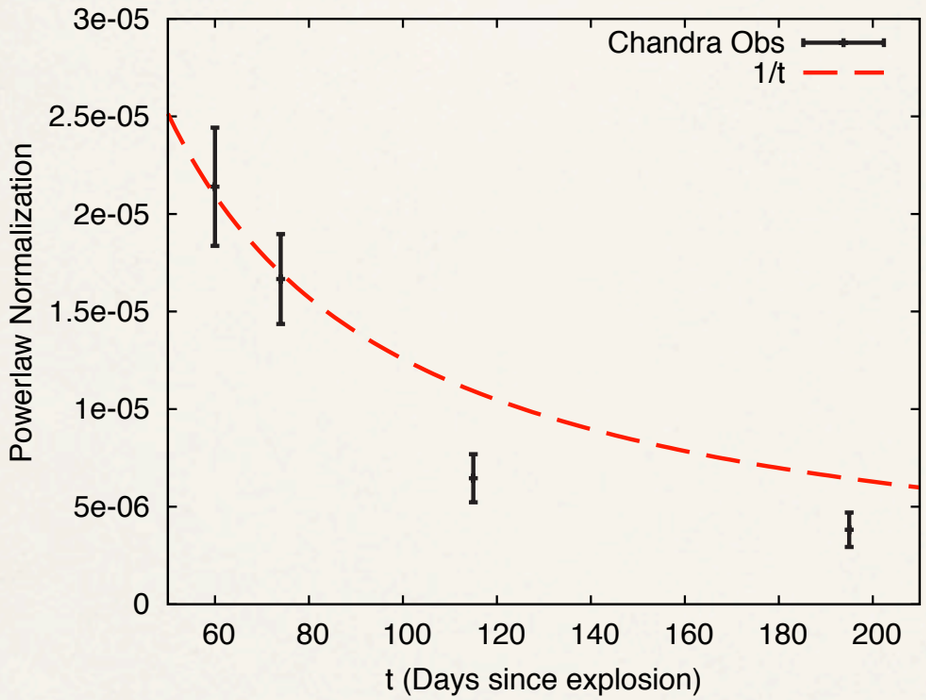

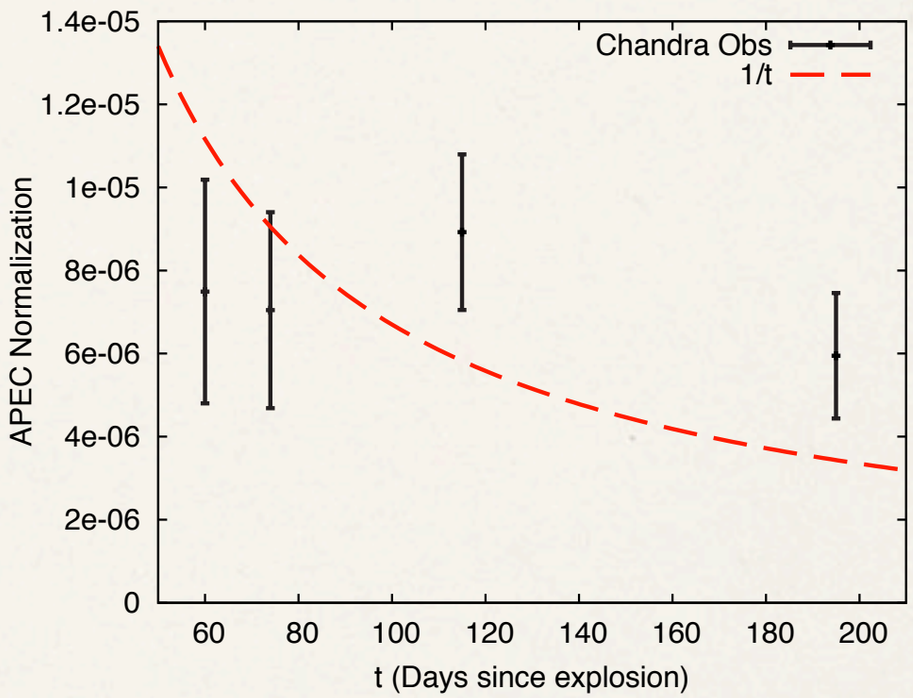

X-ray emission uniquely separable in IC & Thermal components

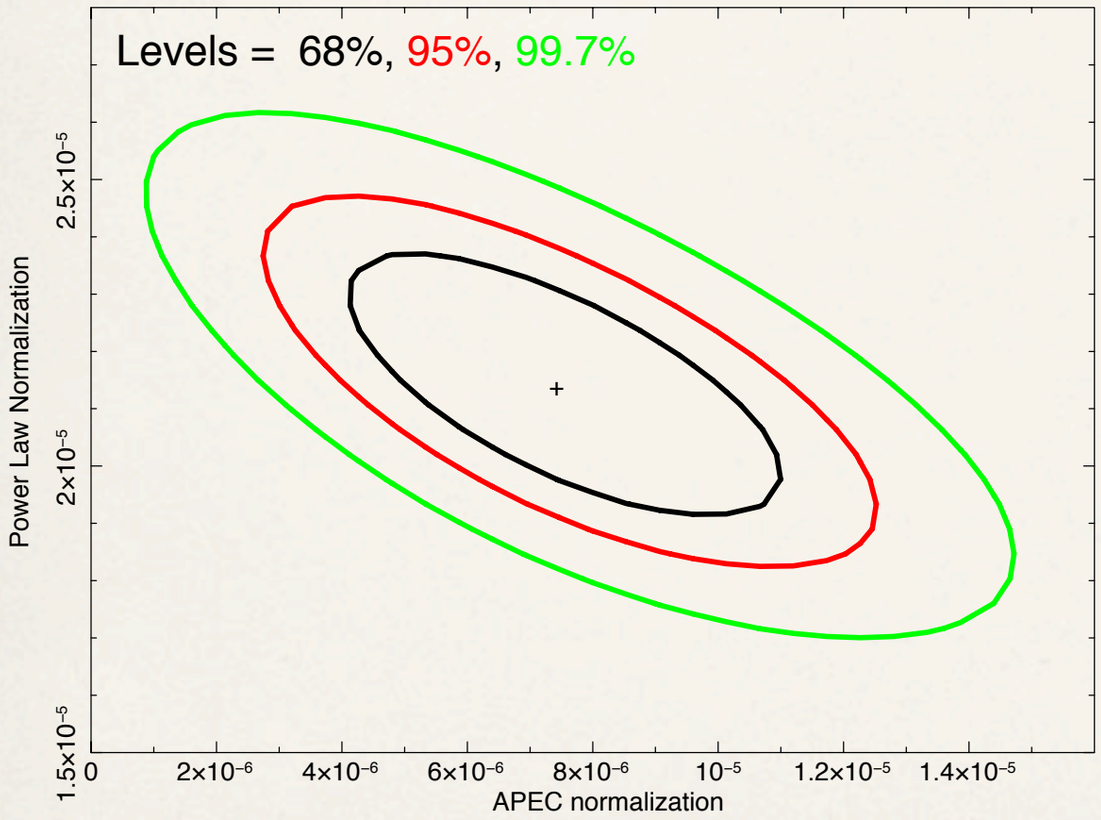

Confidence contours for normalization of the thermal flux (in the *APEC* model) vs. the normalization of the non-thermal flux (in the power-law model). They are anticorrelated and the sum of two fluxes must add up to explain the total observed flux.

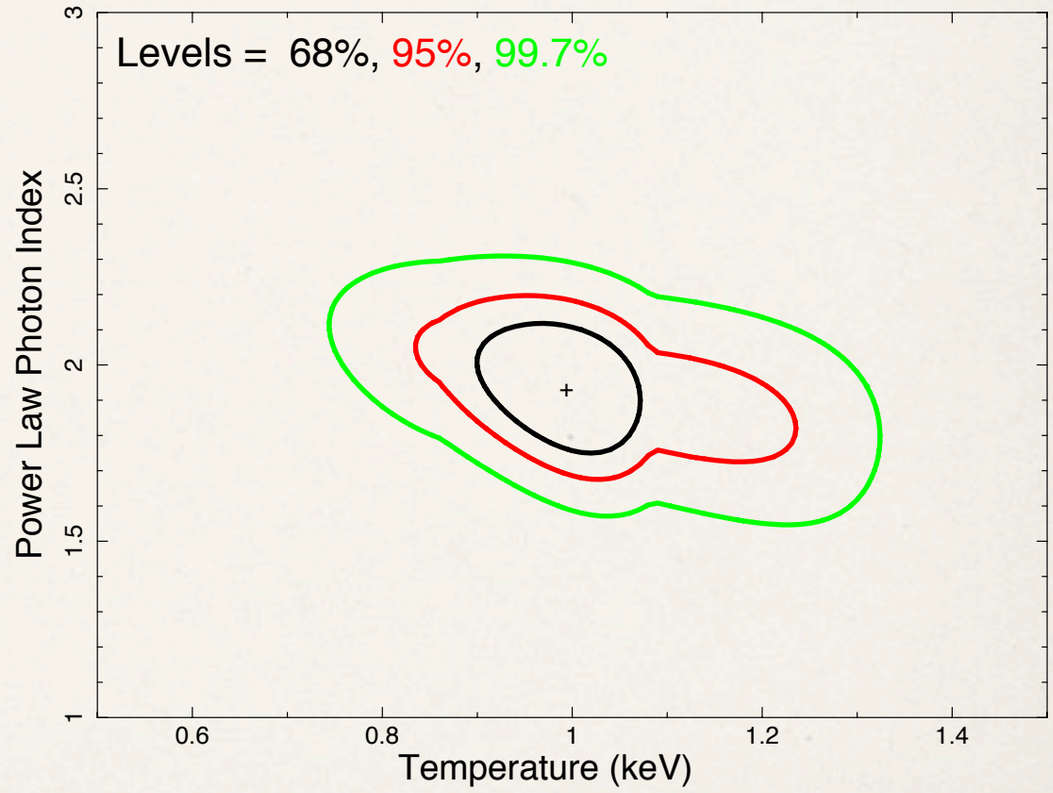

Chandra data successfully breaks the degeneracy between the two components and determine their most important parameters, namely, the temperature and the photon index.

NASA's Astronomy Picture of the Day for March 22, 2012: SN 2012aw

SN 2012aw (arrow) lighting up in spiral galaxy M95; Photo: Adam Block, Mt. Lemmon Center

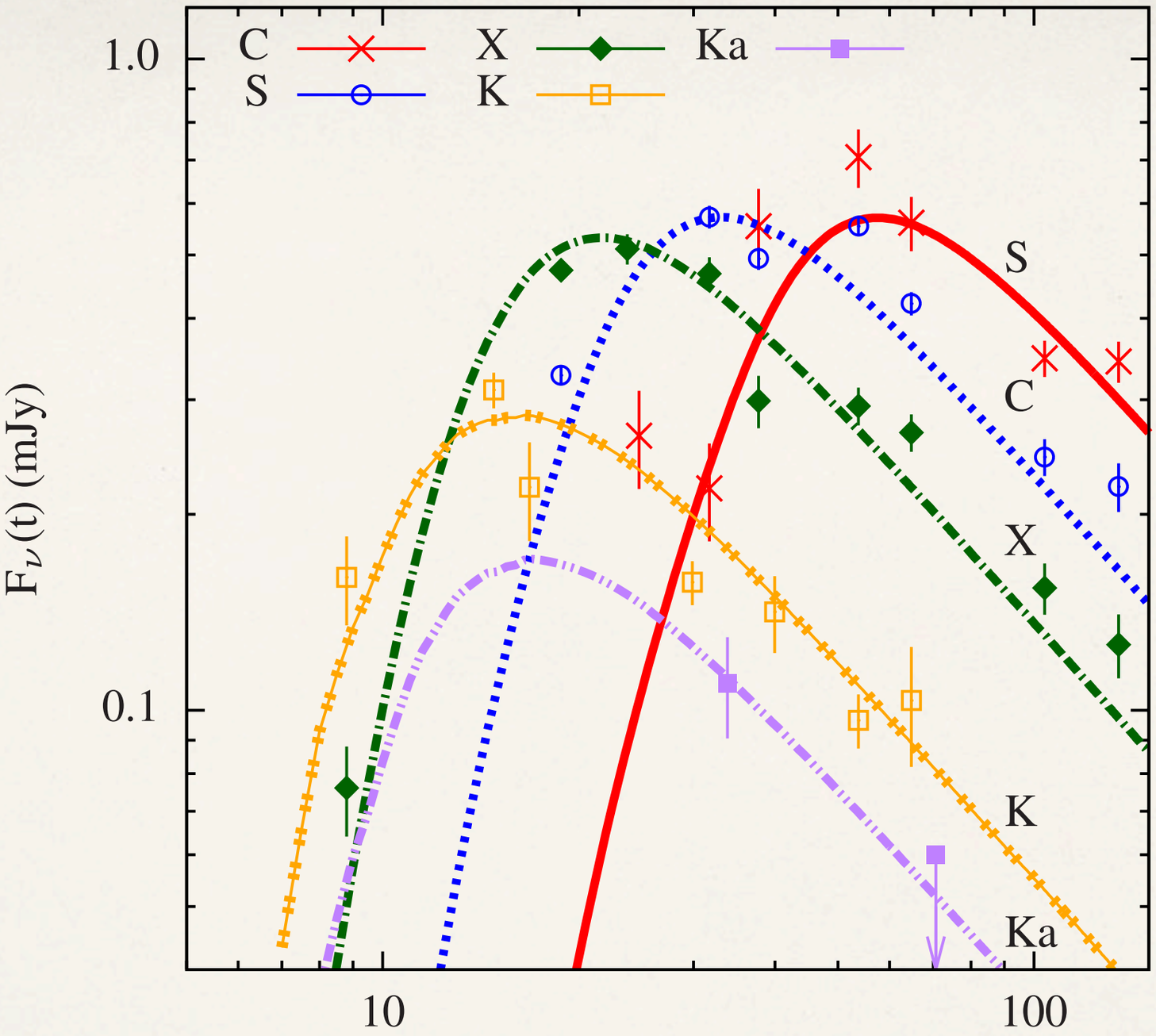

Date of explosion used in this work: March 16.1 2012 UT

First detection: March 16.9, 2012 UT (Fagotti et al). Last non-detection: March 15.27 2012 UT (Poznanski et al)

Evolution of radio spectral indices

$F_\nu \sim \nu^{-\alpha}$

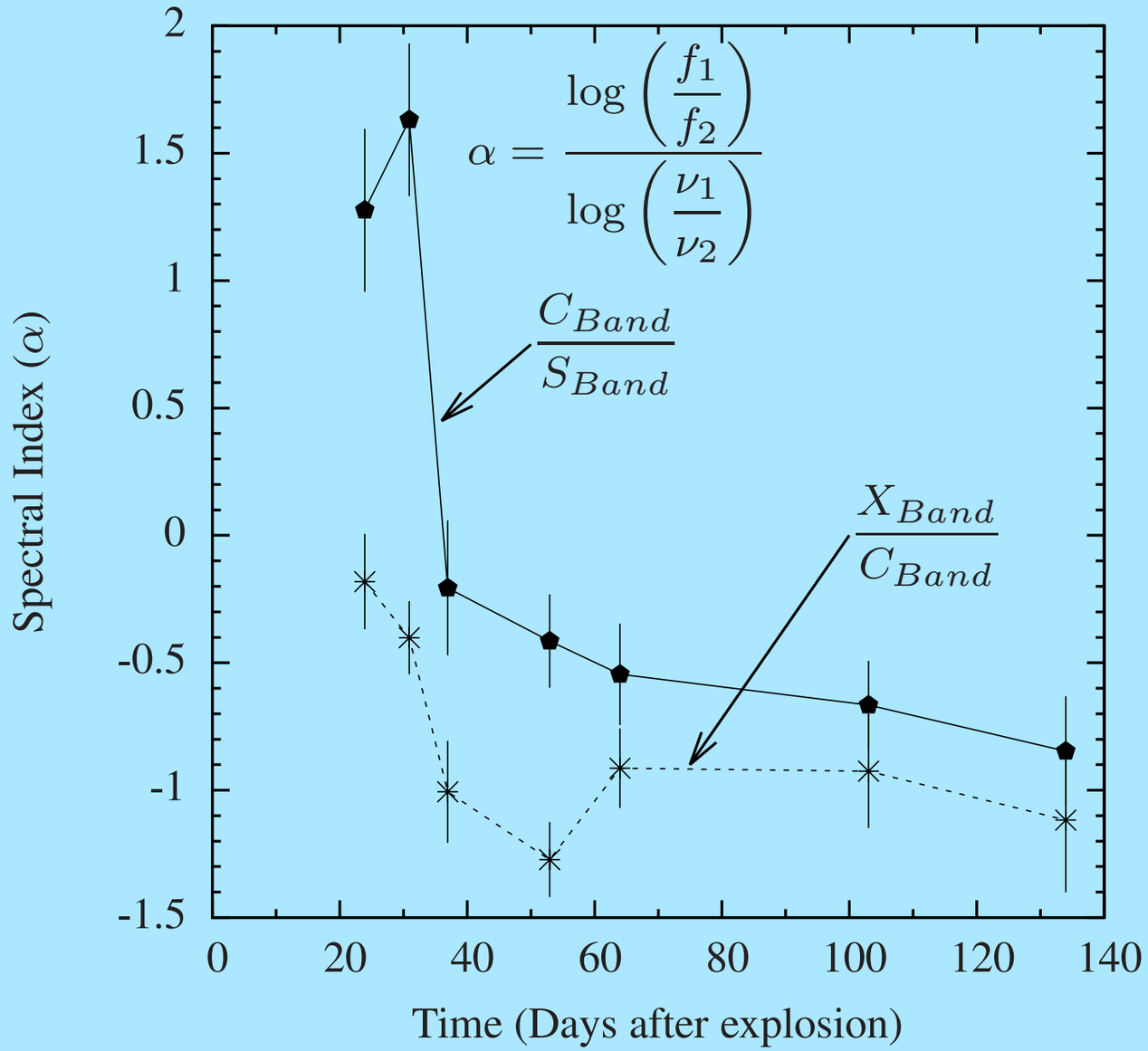

Radio frequencies affected by Inverse Compton Cooling

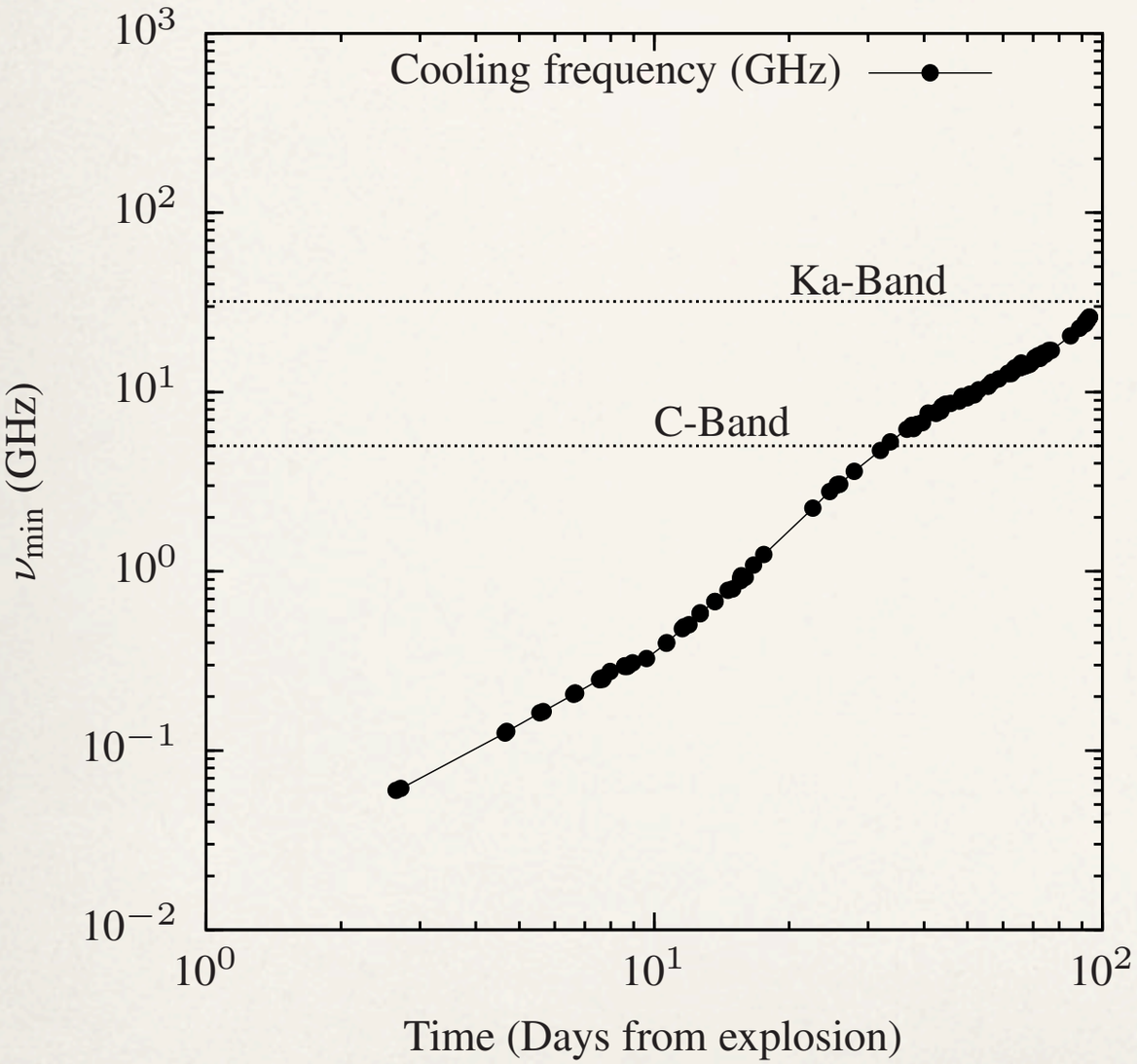

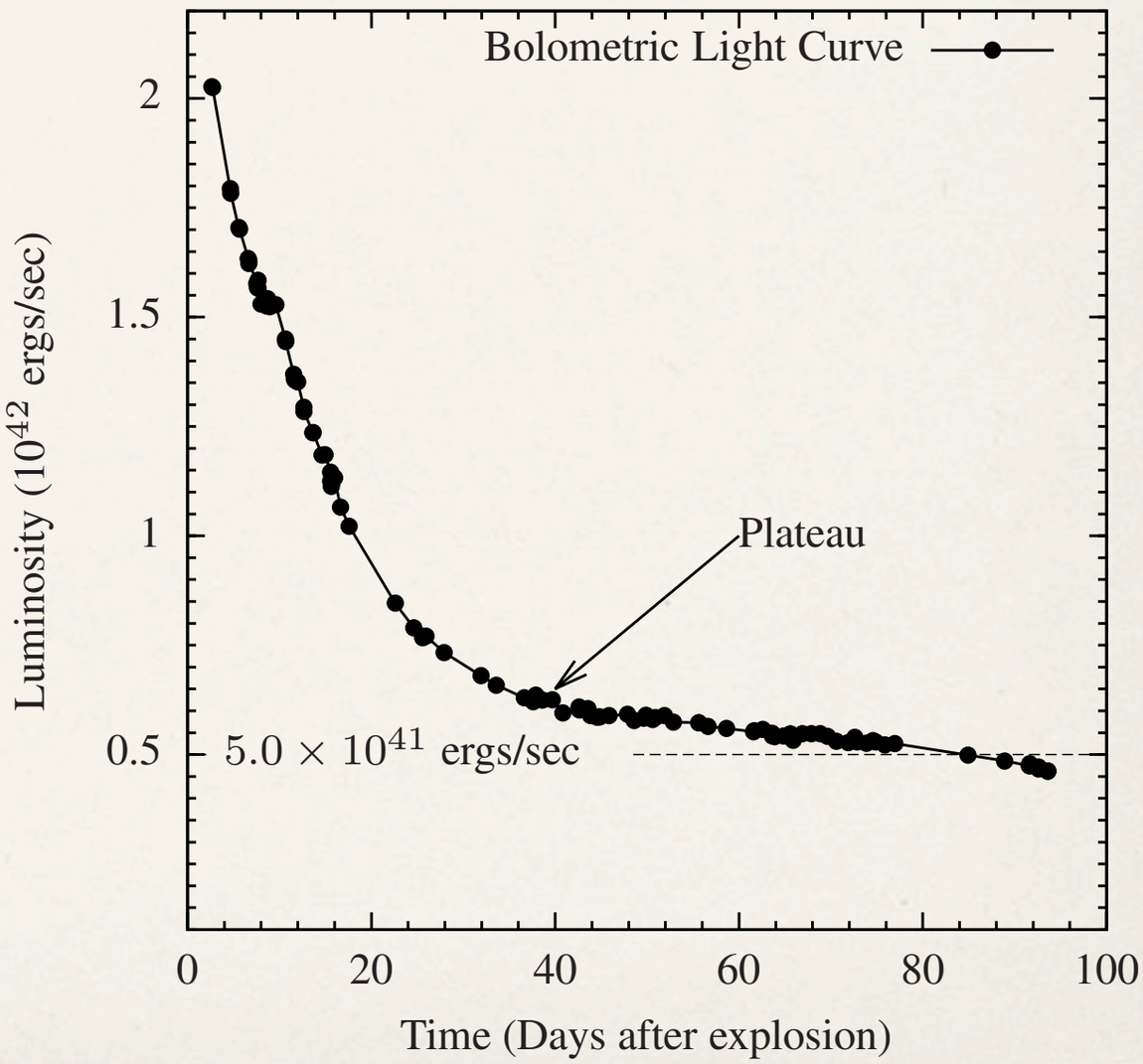

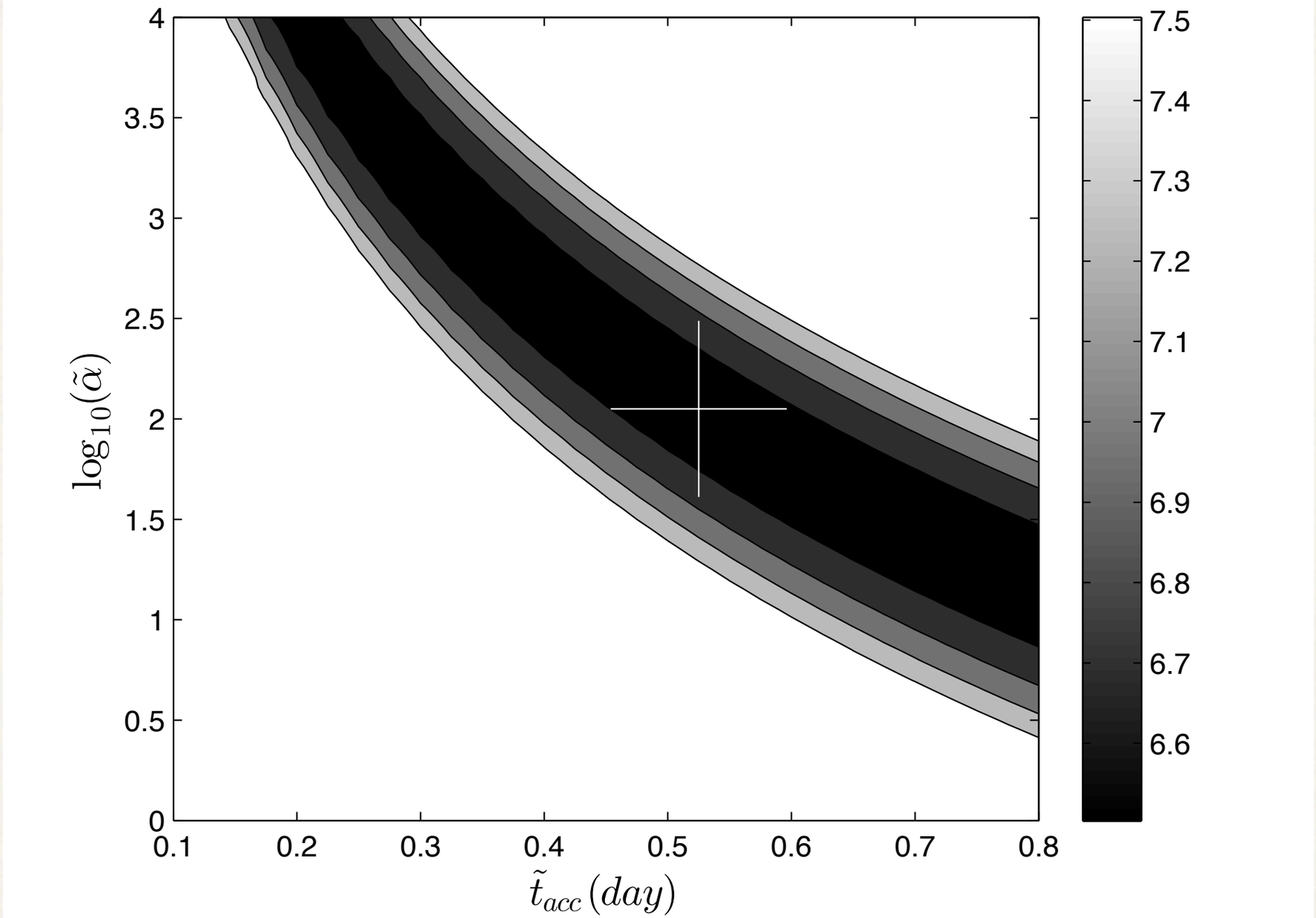
4
3.5
3
2.5
2
1.5
1
0.5
0
0.1
0.2
0.3
0.4
0.5
0.6
0.7
0.8
$\log_{10}(\tilde{\alpha})$
$\tilde{t}_{acc}\,(day)$
7.5
7.4
7.3
7.2
7.1
7
6.9
6.8
6.7
6.6

Summary for radio observations of SN 2012aw

- Radio observations (JVLA & GMRT) of SN 2012aw span 184 days to make it one of the best observed IIP SNe

- Radio spectral index curve at high frequencies shows a dip at early times ($t < 60$ days) & goes below -1, usual for optically thin case

- We show that this is a signature of electron cooling at a young age

- Inverse Compton cooling dominates over Synchrotron cooling because of the abundant seed (optical) photons over the long plateau phase (the long lasting “light bulb”)

- Radiating plasma is far from equipartition => relativistic electrons carry a larger fraction of the thermal energy of the shocked plasma than the post-shock magnetic field.

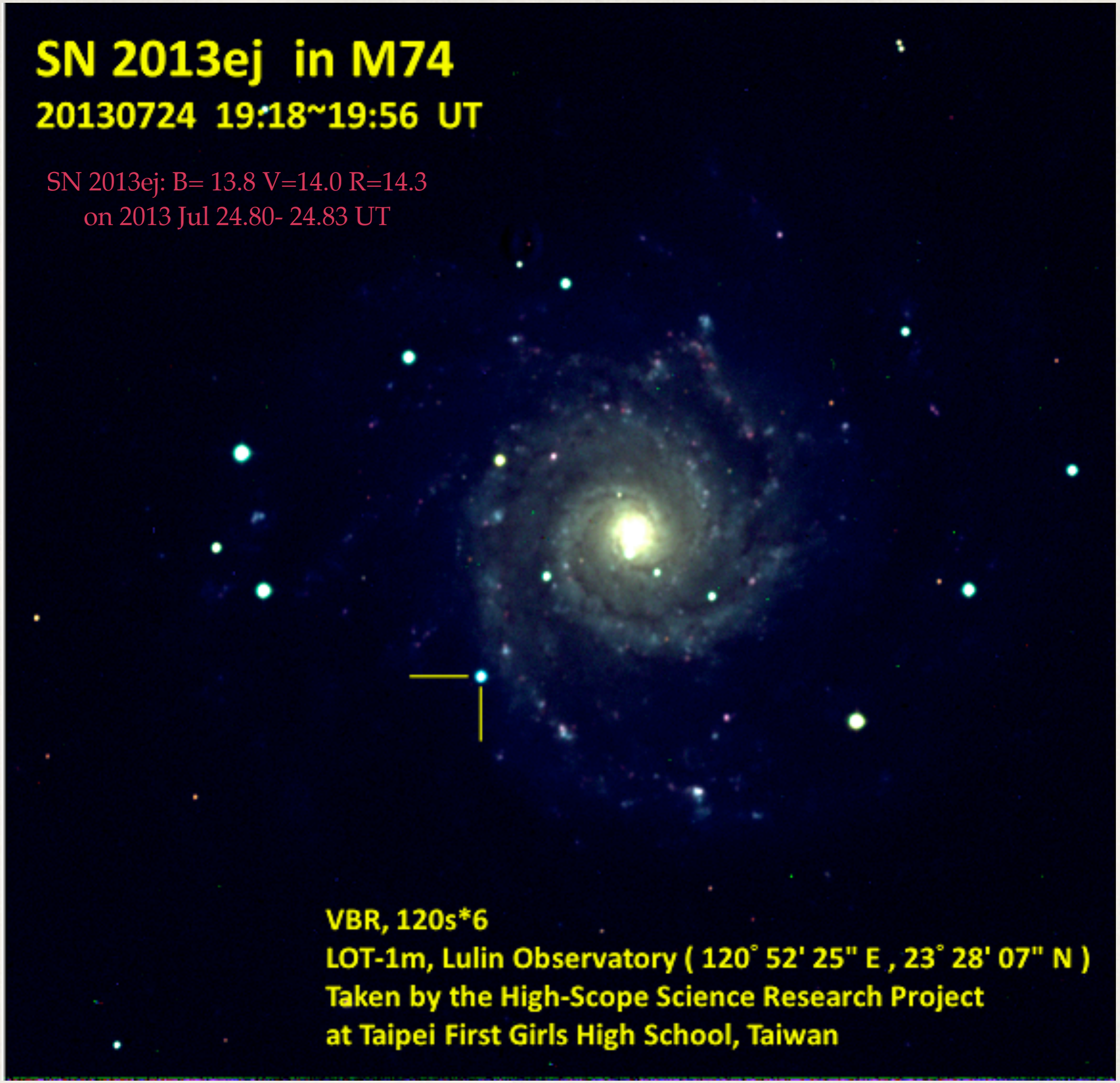
SN 2013ej in M74
20130724 19:18~19:56 UT
SN 2013ej: B= 13.8 V=14.0 R=14.3
on 2013 Jul 24.80- 24.83 UT
VBR, 120s*6
LOT-1m, Lulin Observatory (120° 52' 25" E , 23° 28' 07" N)
Taken by the High-Scope Science Research Project
at Taipei First Girls High School, Taiwan

SN 2013ej in spiral galaxy M74

- M74 is at a distance of 9.1 +/- 1.0 Mpc (Fraser et al 2013).

- From the HST image, Fraser et al (2013) estimate a progenitor mass range of 8 - 15.5 Msun.

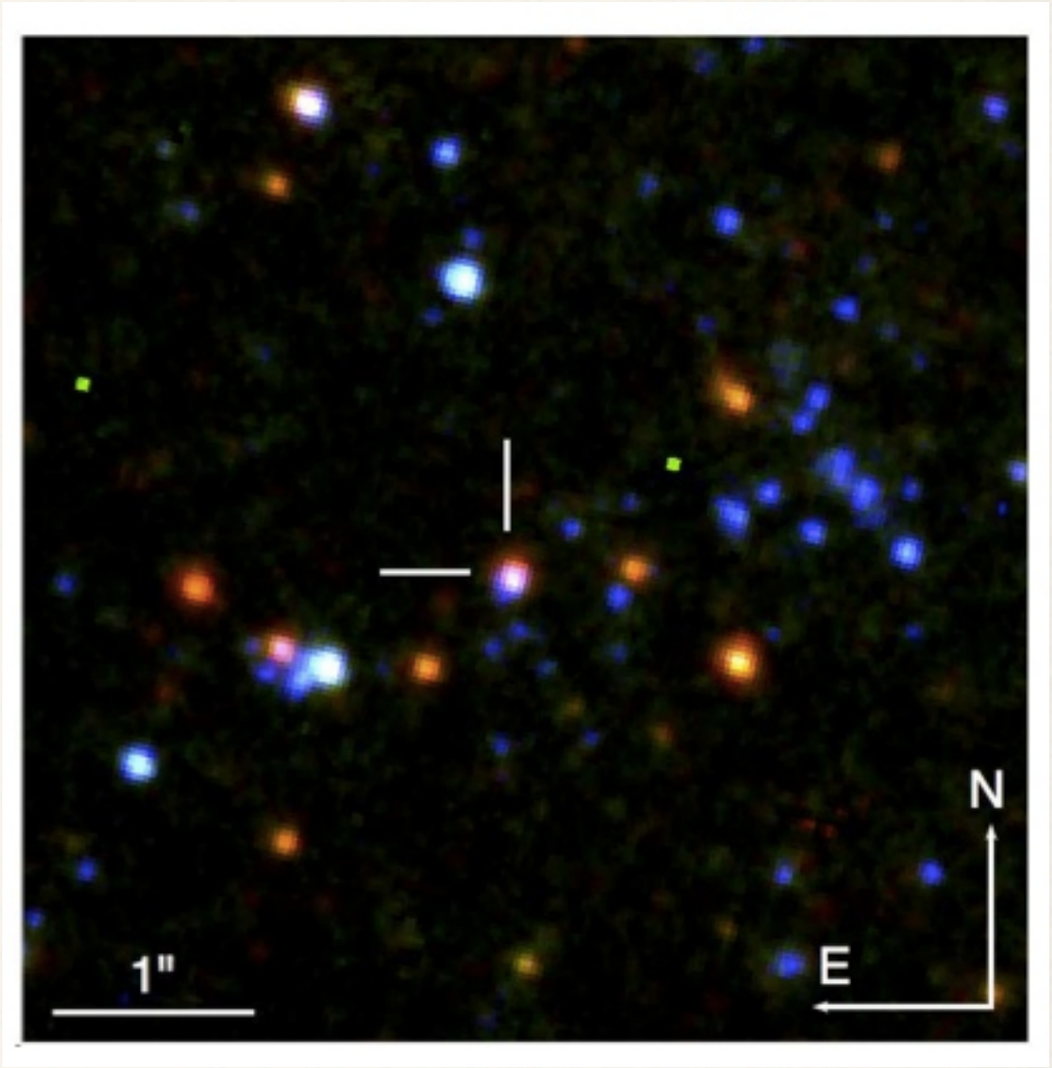

HST ACS image of the site of SN 2013ej prior to explosion (Fraser et al 2013)

Chandra detects SN 2013ej

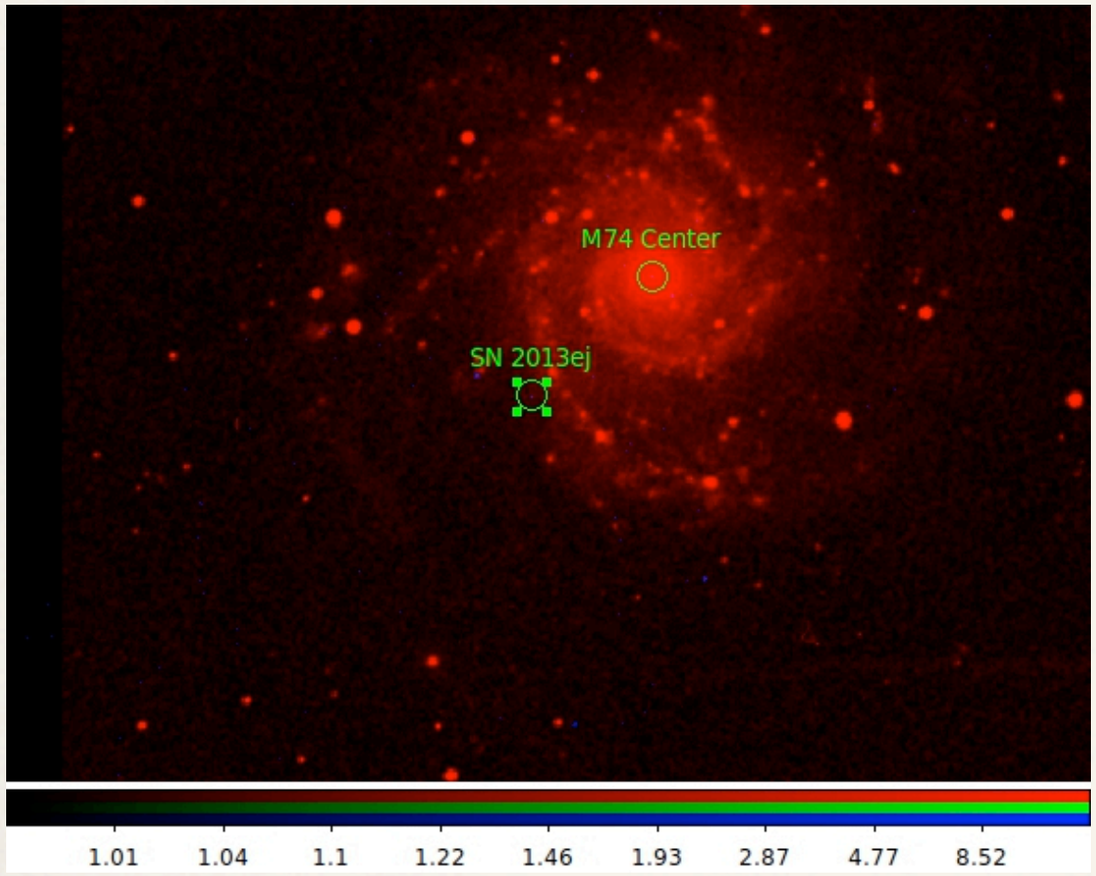

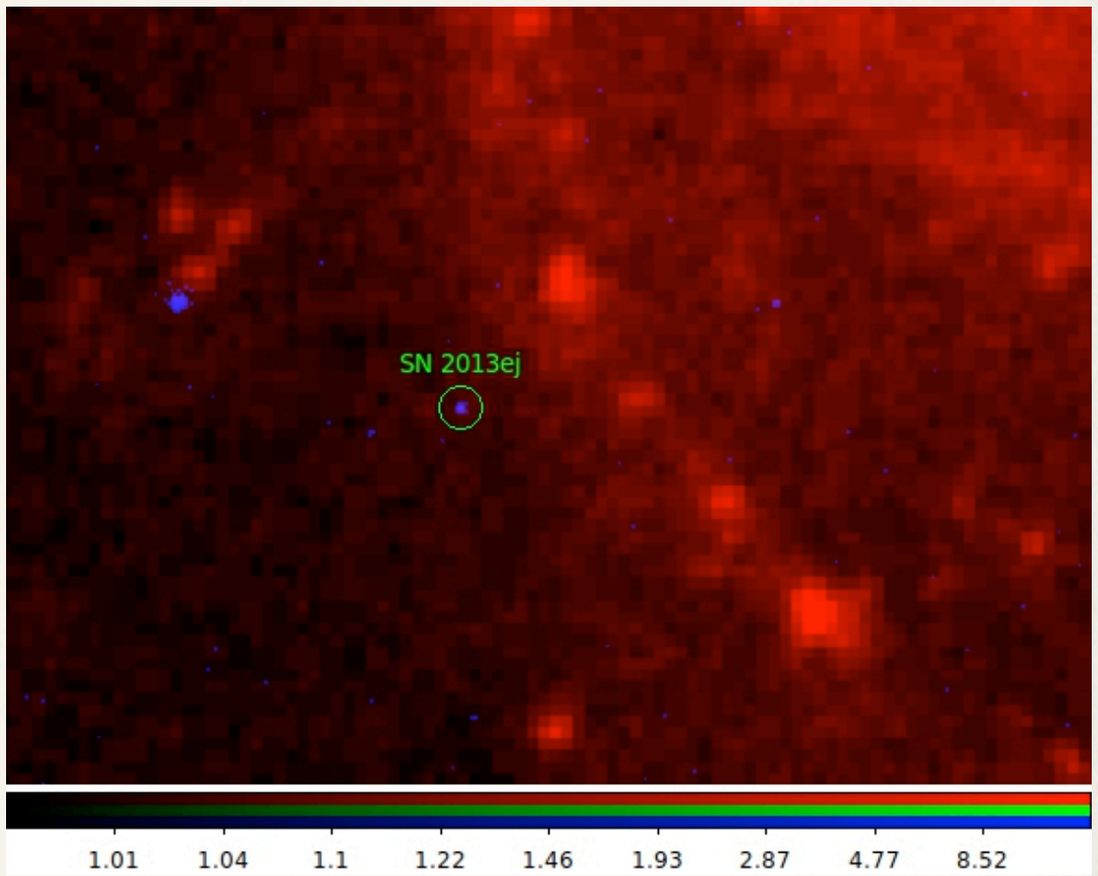

S. Chakraborti, A.R., Keiichi Maeda et al (in prep)

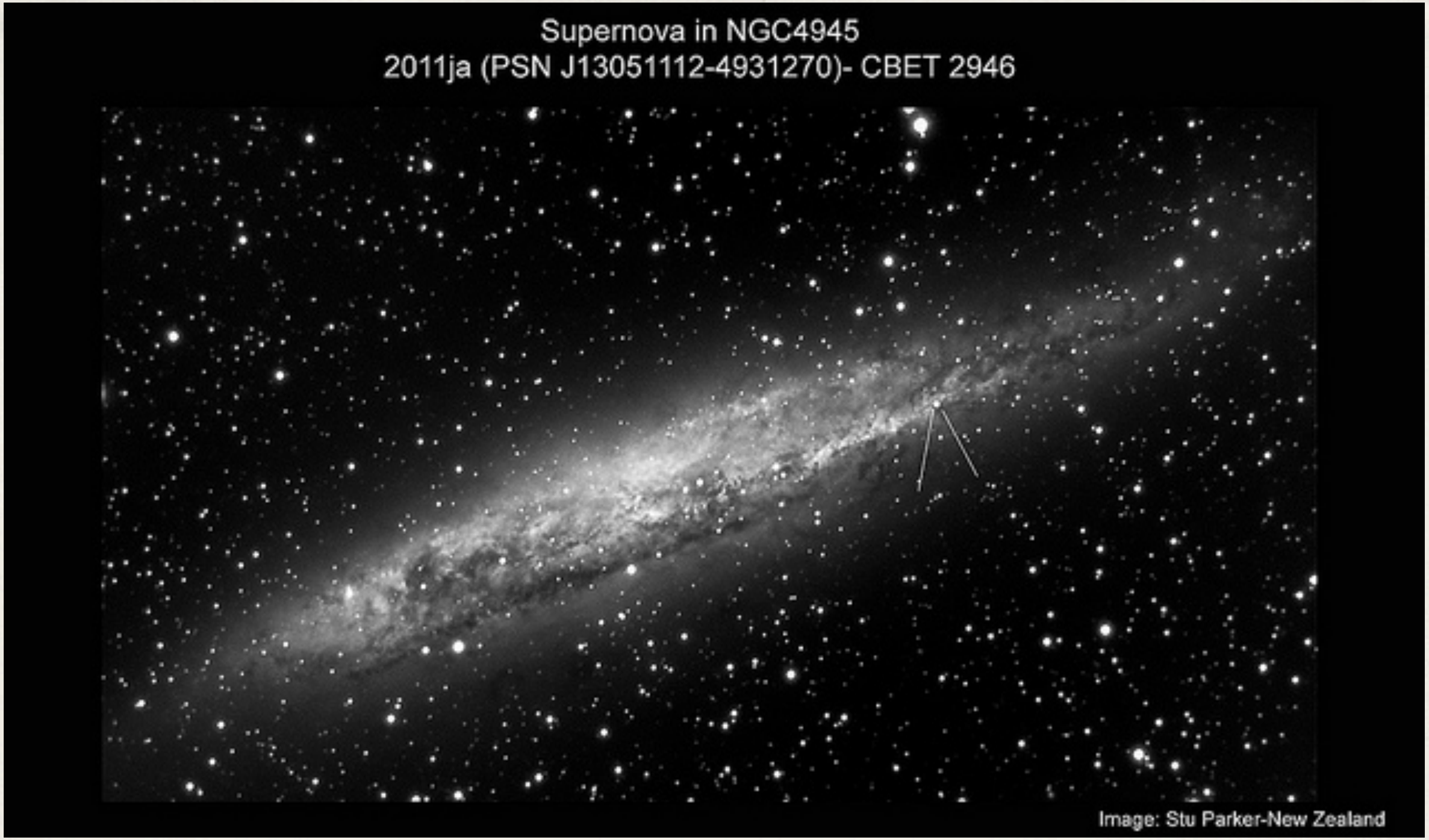

Another Type IIP SN 2011ja

Host galaxy NGC4945 is close by at 3.36 Mpc away (Mouchine et al 2005)

Discovery Magnitude: 14 (unfiltered CCD) On 2011 December 18.1 UT (Monard 2011); Type IIP Classification From Spectra Taken On Dec 19.1 UT (Milisavljevic 2011): Like SN 2004et A Week After Max Light)

Chandra ToO observed SN 2011ja on Jan 10, 2012 & Apr 3, 2012

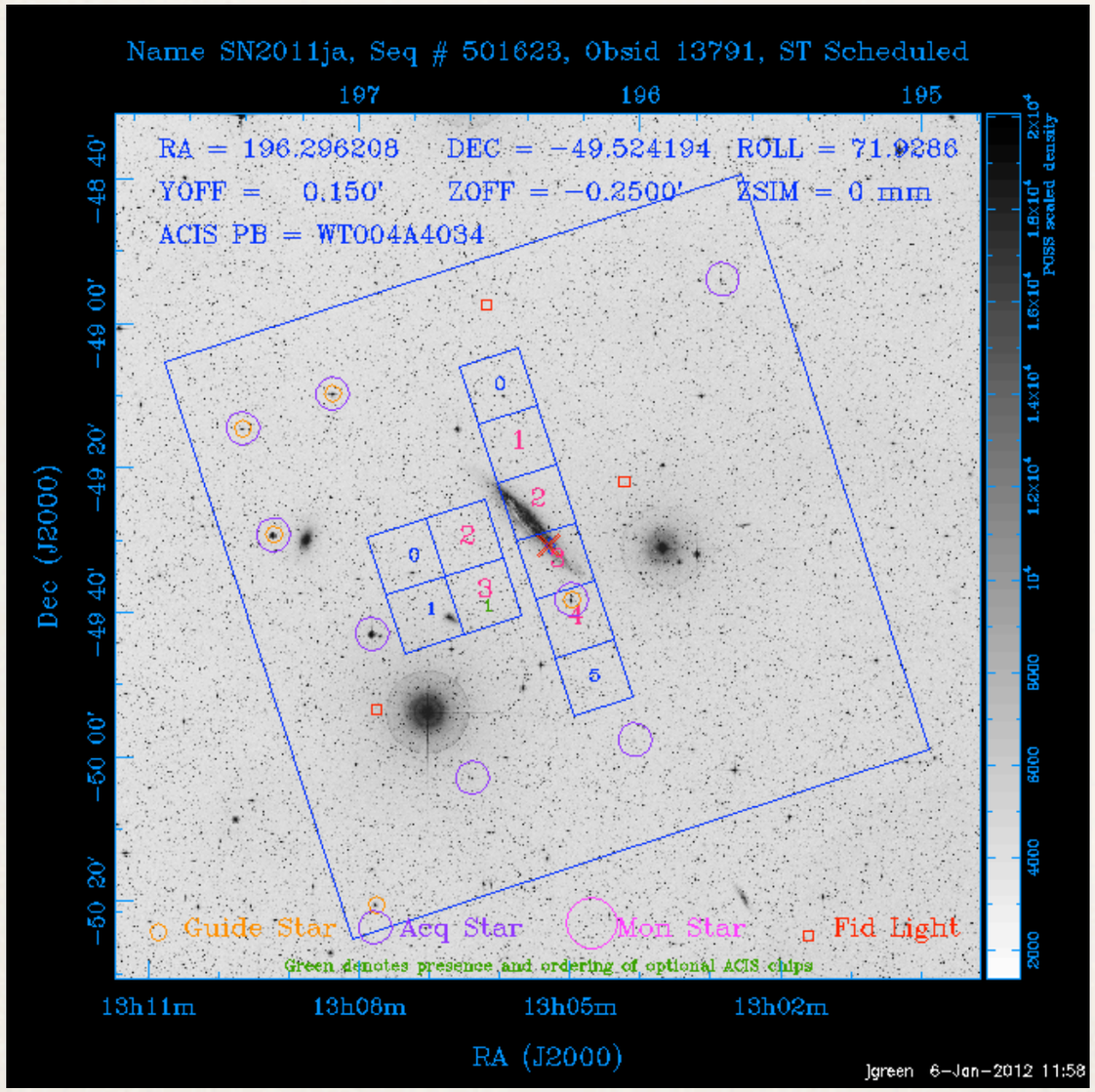

"Target of Opportunity"

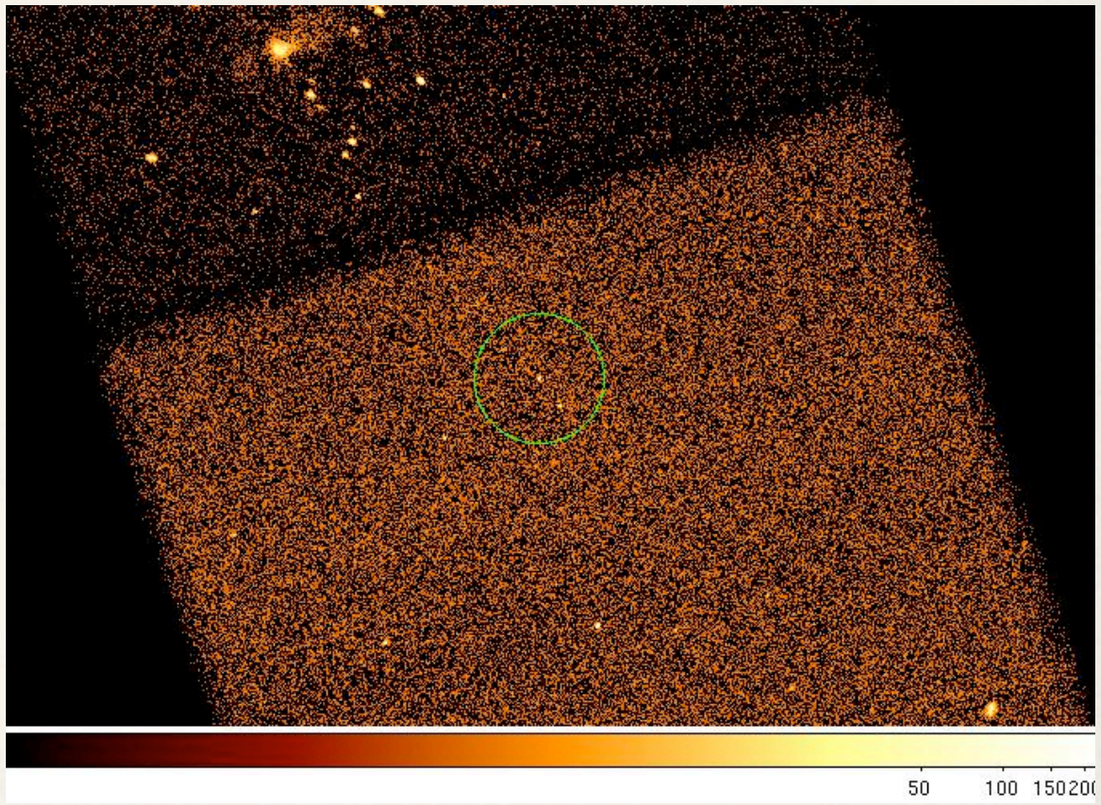

Quick-look image of Jan 10, 2012: detection !

There is another source close-by !

- The contaminating source was present in a pre-SN exposure of the galaxy NGC 4945 on 2000Jan 27.

- It is only 1.35″ away from SN 2011ja

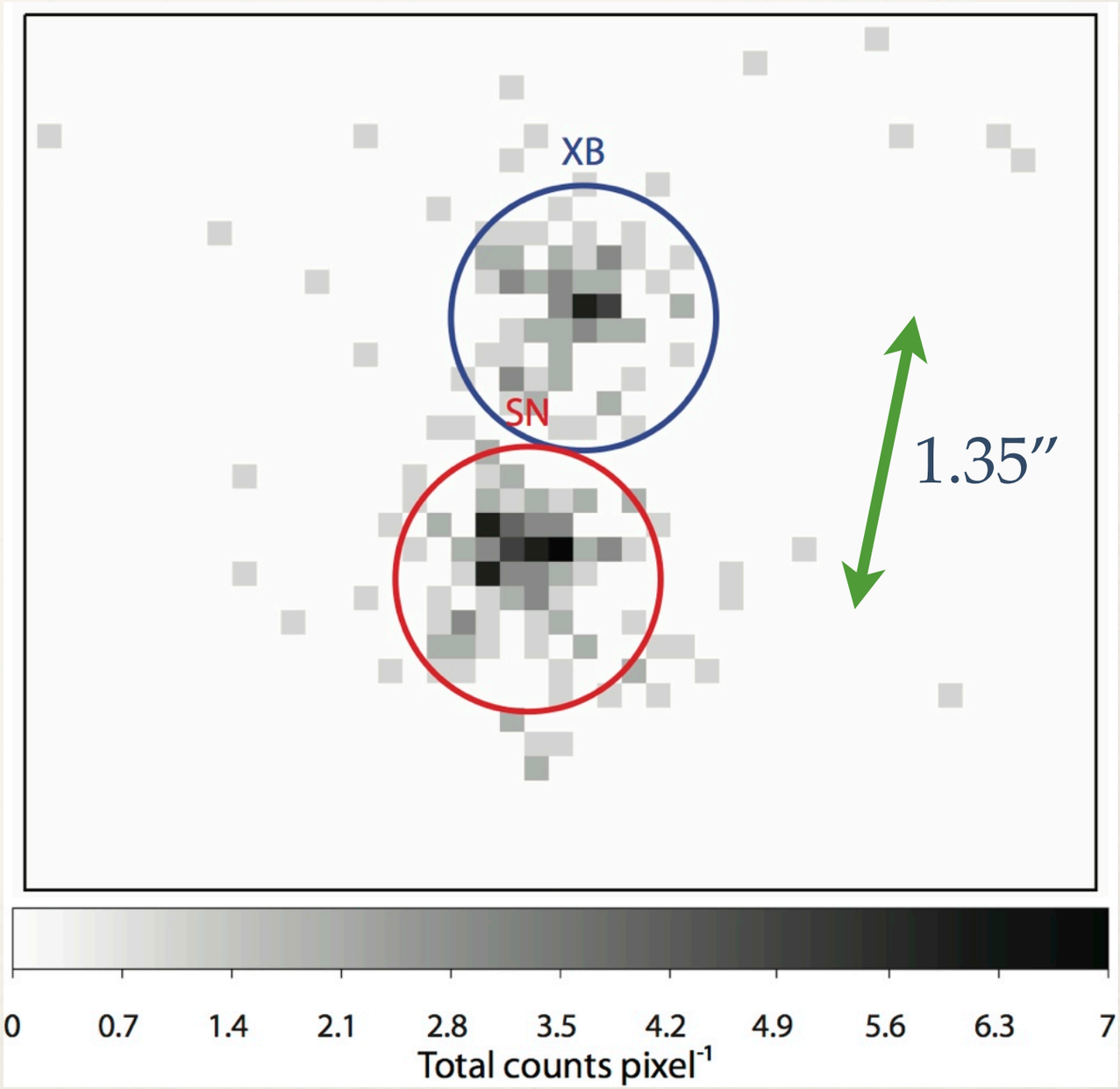

X-ray flux of SN & XB in two epochs

TABLE 1
OBSERVATION OF SN 2011JA WITH CHANDRA

Date	XB Flux (0.3-10 keV) (10^{-14} ergs cm^{-2} s^{-1})	SN Flux (0.3-10 keV) (10^{-14} ergs cm^{-2} s^{-1})
2000 Jan 27	1.01 ± 0.11	none
2012 Jan 10	0.81 ± 0.10	0.98 ± 0.17
2012 Apr 03	1.01 ± 0.11	4.08 ± 0.42

NOTE. — Fluxes are model dependent. X-ray binary is modelled as tbabs(diskbb) and supernova is modeled as tbabs(powerlaw) in XSPEC. See subsection 3.1 for details. Fluxes reported in this table are from the full model and not corrected for absorption.

Chandra X-ray spectra of SN 2011ja at two epochs

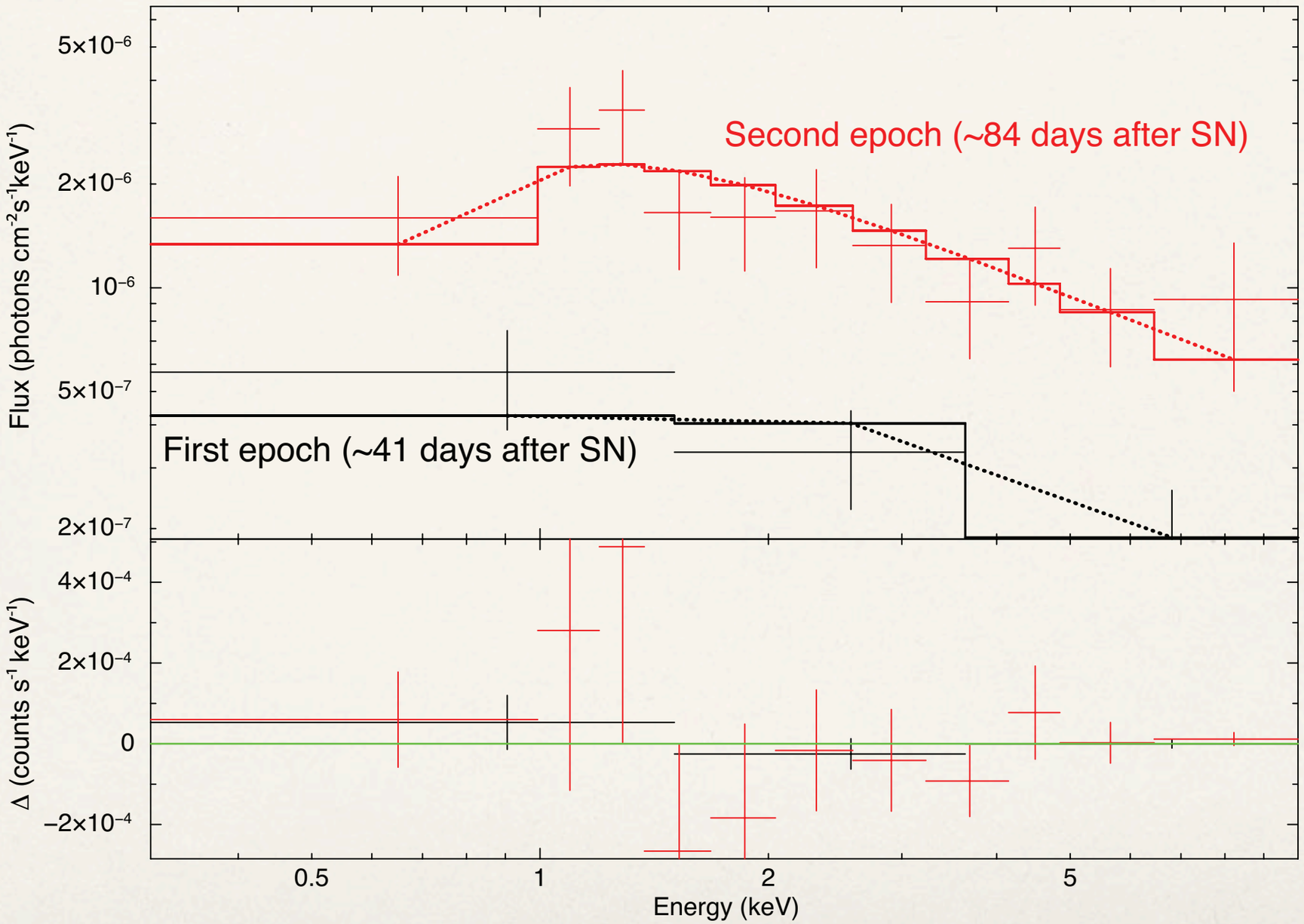

ATCA Radio spectrum:
2011 Dec 19

- Radio emission due to Synchrotron radiation.
- Assuming Synchrotron self absorption model at late times:

$$R_s = 4.0 \times 10^{14} \alpha^{-1/19} \left(\frac{f}{0.5}\right)^{-1/19} \left(\frac{F_p}{\mathrm{mJy}}\right)^{9/19} \times \left(\frac{D}{\mathrm{Mpc}}\right)^{18/19} \left(\frac{\nu}{5\ \mathrm{GHz}}\right)^{-1} \mathrm{cm},$$

- Under equipartition, $R_s = 1.8 \times 10^{15}$ cm
- Expansion velocity from Halpha absorption minimum: 11,000 km/s (Milisavljevic 2011) => age 19.4 days at time of radio obs (Dec 19).
- Explosion date: 2011 Nov 30 UT (+/- 2 days)

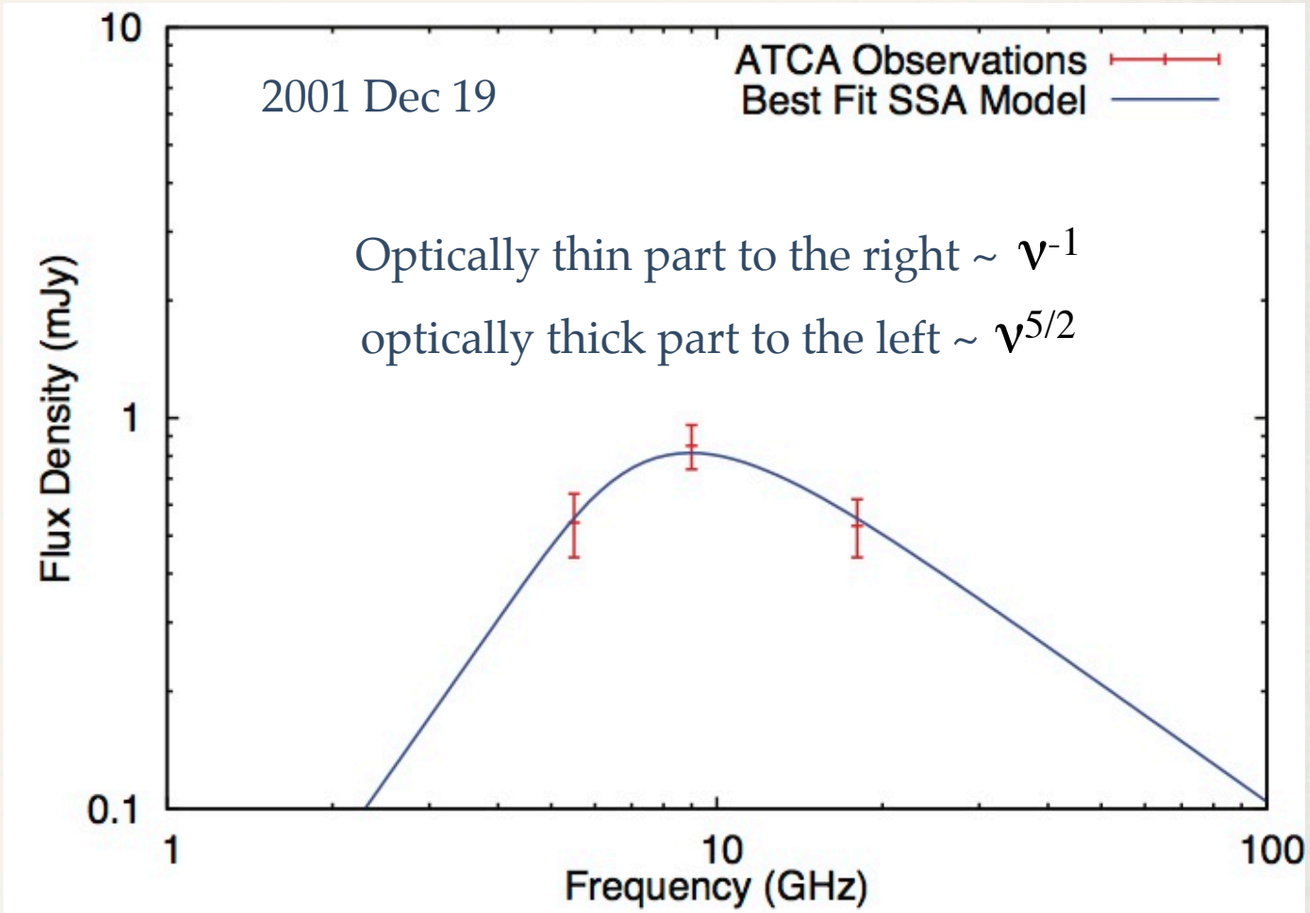

Varying mass loss rate of the progenitor of SN 2011ja: complex circumstellar medium set up by a non-steady wind?

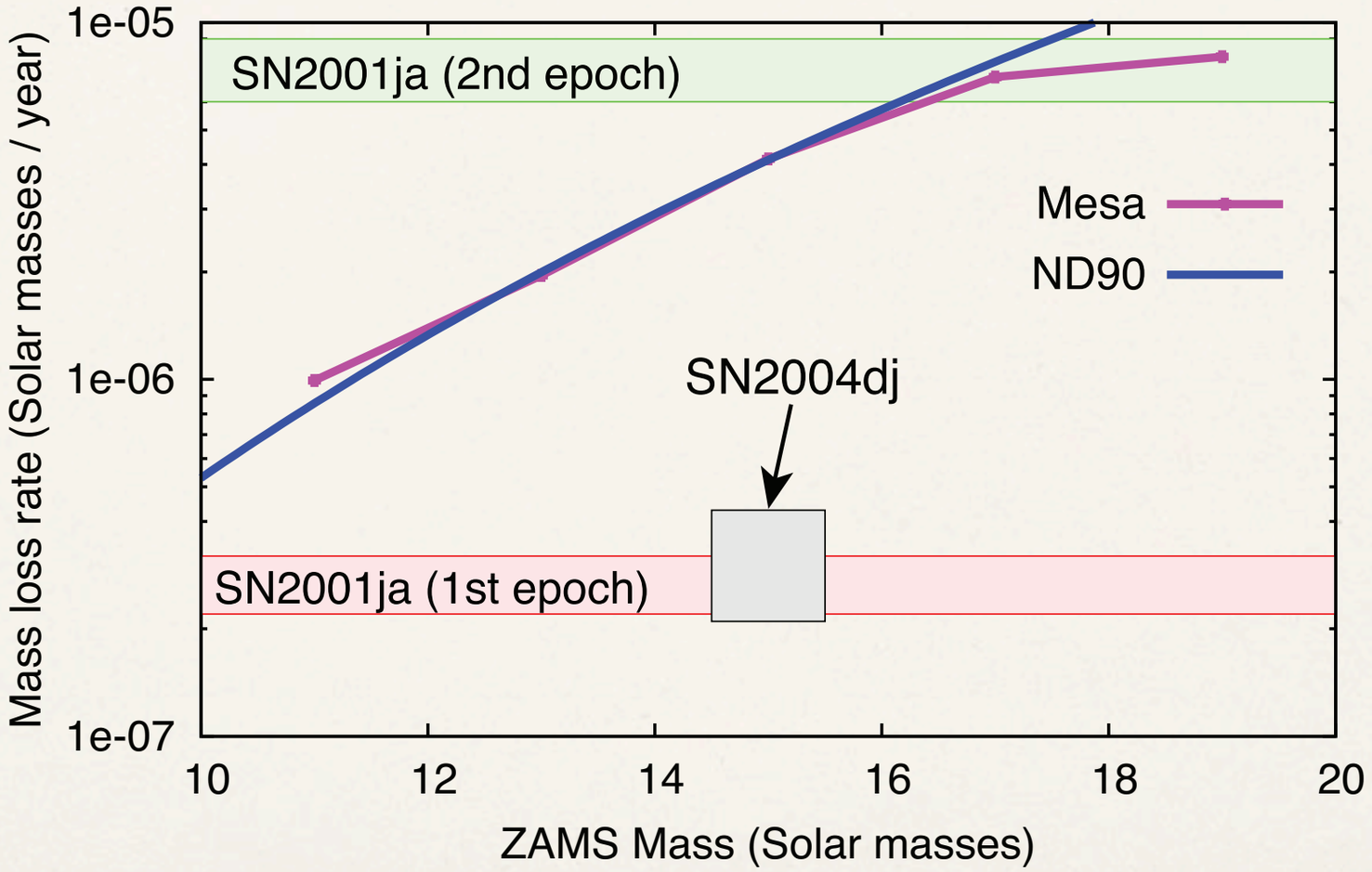

Summary & Conclusions

- X-rays in SN 2004dj: a combination of thermal and non-thermal processes. At early spectra dominated by Inverse Compton scattering by relativistic electrons of optical SN photons at the forward shock. X-ray luminosity falls off as L_{bol}/t. At late time dominant emission is from reverse shock heated thermal plasma which falls off as $1/t$

- Radio observations (JVLA & GMRT) of SN 2012aw show its radio spectral index curve at high frequencies has a dip at early times ($t < 60$ days). This is an indication of electron cooling. Inverse Compton cooling dominates over Synchrotron cooling because of the abundant seed (optical) photons over the long plateau phase (the long lasting "light bulb")

- Radiating plasma in SN 2012aw is far from equipartition => relativistic electrons carry a larger fraction of the thermal energy of the shocked plasma than the post-shock magnetic field. However, for SN 2004dj, around a third of the energy thermalized by the collision of the ejecta with circumstellar matter is used to accelerate electrons to relativistic velocities and about a tenth of the thermal energy available is used in the turbulent amplification of magnetic fields. ε_B and ε_e are determined separately by the use of X-ray, radio and optical data.

Thank You

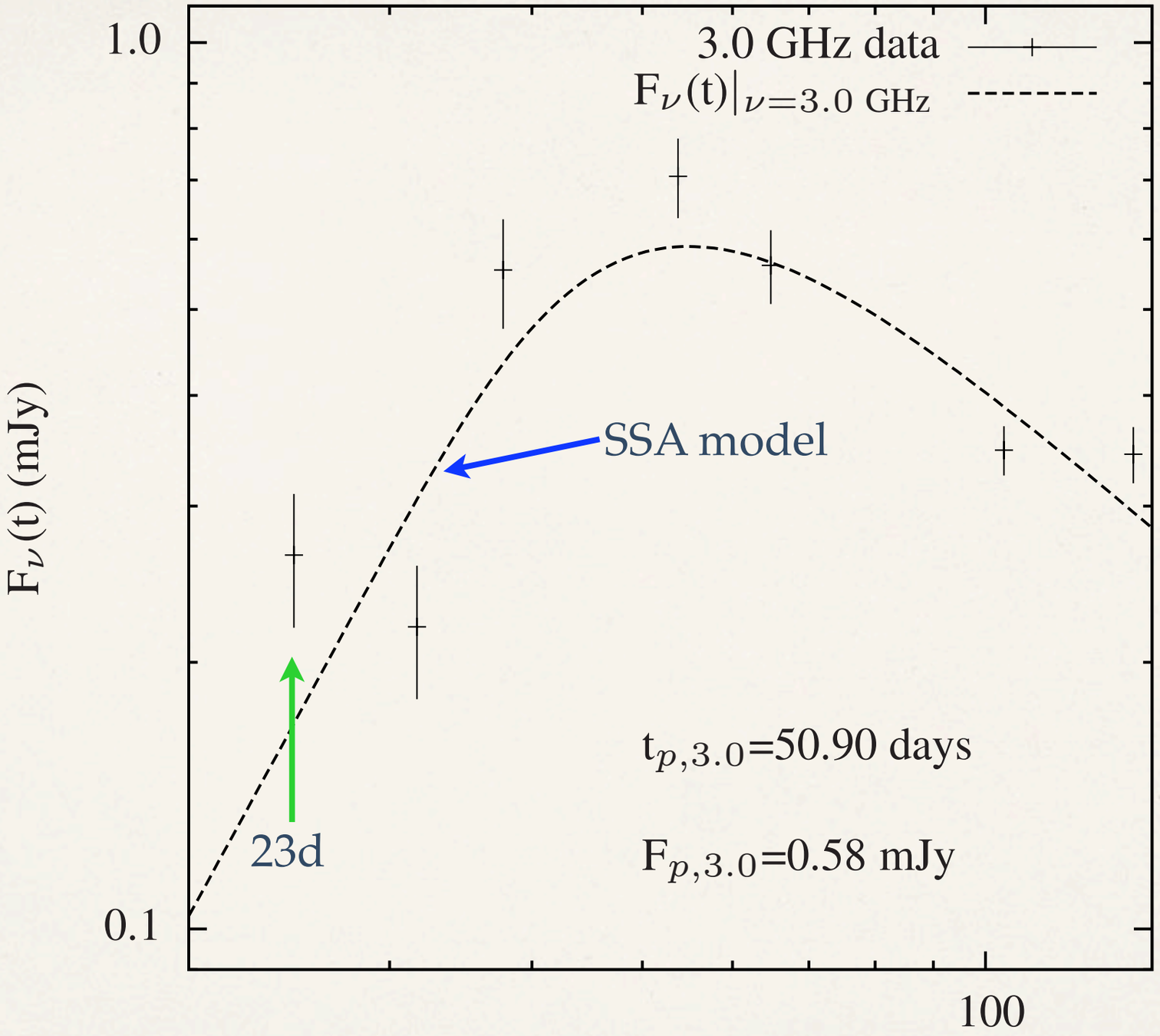

Chevalier (1998) model gives $R_0 = 3.9 \times 10^{15}$ cm & $B_0 = 0.48$ G at t ~50.9 d

IC cooling & radio frequency turnover

Electrons affected by cooling ($t_{IC} < t_{Ad}$) have energy greater than:

$$E > \frac{1}{3.97 \times 10^{-2} u_{rad} \times 1.5t}$$

With $\nu_C \sim const \times B\, E^2$, minimum radio frequency above which Compton cooling present:

$$\begin{aligned} \nu_{min} &\gtrsim \frac{c_1 B_0}{t_0^3} \times \left(\frac{4\pi R_0^2 c}{5.96 \times 10^{-2}} \right)^2 \times \left(\frac{t}{L_{bol}^2} \right) \\ &= 89.5 \left(\frac{t}{10 \text{ days}} \right) \left(\frac{L_{Bol}}{10^{42}} \right)^{-2} \text{ GHz} \end{aligned}$$

Electron energy distribution has a truncation point depending upon the loss and gain terms affecting individual electron energy:

$$\frac{dE}{dt} = \left(\frac{dE}{dt} \right)_+ - \left(\frac{dE}{dt} \right)_-$$

Radio light curve from electron distribution and model calculation

Radio flux density calculated in terms of the source function $S_\nu = \varepsilon_\nu / \varkappa_\nu$ with free-free absorption (Chevalier 1998):

$$F_\nu = S_\nu \Omega (1 - e^{-\tau_\nu}) \times \exp\left\{ - \left(\frac{t}{t_{ff}}\right)^{-3} \left(\frac{\nu}{\nu_1}\right)^{-2.1} \right\}$$

t_{ff} is the time at which optical depth to FFA becomes unity at radio frequency ν_1

Compute the radio fluxes as a function of time, with:

1. For a given explosion date (t_{ex}) fit the 3 GHz light curve with an SSA model to determine peak values of F_p, t_p and m (where $R(t) = R_0(t)\ (t/t_0)^m$).
2. Calculate the radius R_p & B_p from SSA model expressions using F_p, t_p .
3. Use R_p, B_p & t_p in the cooling model to calculate the best fit values of t_{ff} , t_{acc} & log ($\underline{\alpha}$) based on χ^2 minimization.
4. Use optical light curves referenced to explosion dates to compute the cooling model

The best fit from radio data gives:

$$t_{ff} = 18.5 \text{ days},\ \tilde{t}_{acc} = 0.53 \text{ days and } \tilde{\alpha} = 1.12 \times 10^2 \qquad \tilde{\alpha} = \epsilon_e / \epsilon_B$$

Another method to obtain the equipartition factor α:

Integrate the spectral distribution of the X-ray luminosity expected from IC (Chakraborti et al 2012) for 0.5-2.0 keV; relate the observed X-ray luminosity & radio emission measure:

$$5.28 \times 10^{36} \gamma_{min} S_\star \tilde{\alpha}^{11/19} V_{s4} \left(\frac{L_{bol}(t)}{10^{42}\ \mathrm{ergs}^{-1}}\right) \left(\frac{t}{10\ \mathrm{days}}\right)^{-1} \lesssim L^X_{obs}$$

$$S_\star = 1.0 \left(\frac{f}{0.5}\right)^{-8/19} \left(\frac{F_{\nu p}}{\mathrm{mJy}}\right)^{-4/19} \left(\frac{D}{\mathrm{Mpc}}\right)^{-8/19} \left(\frac{\nu}{5\ \mathrm{GHz}}\right)^{2} \left(\frac{t}{10\ \mathrm{days}}\right)^{2}$$

Chandra observed SN 2012aw on 2012 Apr 11. Luminosity: (6 +/- 1.4) x 10^{37} erg/s/keV. This value implies an equipartition factor from above:

$$\tilde{\alpha} \sim 0.26 \times 10^2$$

Electron energy distribution:

Electron distribution function at time t (Pacholczyk 1970) is:

$$N(E,t) = \begin{cases} N_0 E^{-\gamma}\left(1-\frac{E}{E_{max}}\right)^{\gamma-2} & E_{min} < E < E_{max} \\ 0 & E > E_{max} \end{cases}$$

$$E_{min} = m_e c^2$$

Electrons are accelerated by SN shock and gain energy and lose energy by radiative processes, e.g. IC. The maximum electron energy E_{max} is dependent upon the shock radius and bolometric luminosity (supply of seed photons):

$$E_{max} = \frac{4\pi R(t)^2 c}{3.97 \times 10^{-2} \tilde{t}_{acc} L_{bol}(t)}$$

Normalization N_0 is related to the equipartition factor $\underline{\alpha}$:

$$N_0 = \frac{\tilde{\alpha}(\gamma-2)B^2 E_{min}^{\gamma-2}}{8\pi}$$

Electron energy & Inverse Compton scattering

- Rates at which an electron loses energy:

$$\left(\frac{dE}{dt}\right)_A \approx \frac{2}{3}Et$$

Adiabatic loss

$$\left(\frac{dE}{dt}\right)_{IC} \propto u_{rad}E^2$$

Inverse Compton cooling

$$\left(\frac{dE}{dt}\right)_{SC} \propto B^2E^2$$

Synchrotron

- Timescales:

$$t_{IC} = \frac{1}{3.97 \times 10^{-2} u_{rad} E}$$

$$t_{SC} = \frac{1}{5.95 \times 10^{-2} u_B E}$$

$$u_{rad}(t) = \frac{L_{Bol}(t)}{4\pi R(t)^2 c}$$

Radiation density at the radiosphere

IC & radio emission measures

Ejecta with density profile runs into a steady (s=2) wind of the presupernova star:

$$\rho_{\rm ej} \propto t^{-3} V^{-\eta}$$

$$\rho_{\rm w} = \frac{A}{r^2} = \frac{\dot{M}}{4\pi r^2 v_{\rm w}}$$

Chevalier & Fransson 2006:

$$E\frac{dL_{\rm IC}}{dE} \approx 8.8 \times 10^{36} \gamma_{\rm min} S_\star \alpha^{11/19} V_4 \times \left(\frac{L_{\rm bol}(t)}{10^{42}\,{\rm erg\,s^{-1}}}\right) t_{10}^{-1}\,{\rm erg\,s^{-1}}$$

$\alpha \equiv \epsilon_e/\epsilon_B$

in terms of the radio emission measure

$$S_\star = A_\star \epsilon_{B-1} \alpha^{8/19} = 1.0 \left(\frac{f}{0.5}\right)^{-8/19} \left(\frac{F_{\rm p}}{\rm mJy}\right)^{-4/19} \times \left(\frac{D}{\rm Mpc}\right)^{-8/19} \left(\frac{\nu}{5\,{\rm GHz}}\right)^{-4/19} t_{10}^2,$$

Ugliano, Janka et al 2012 ApJ

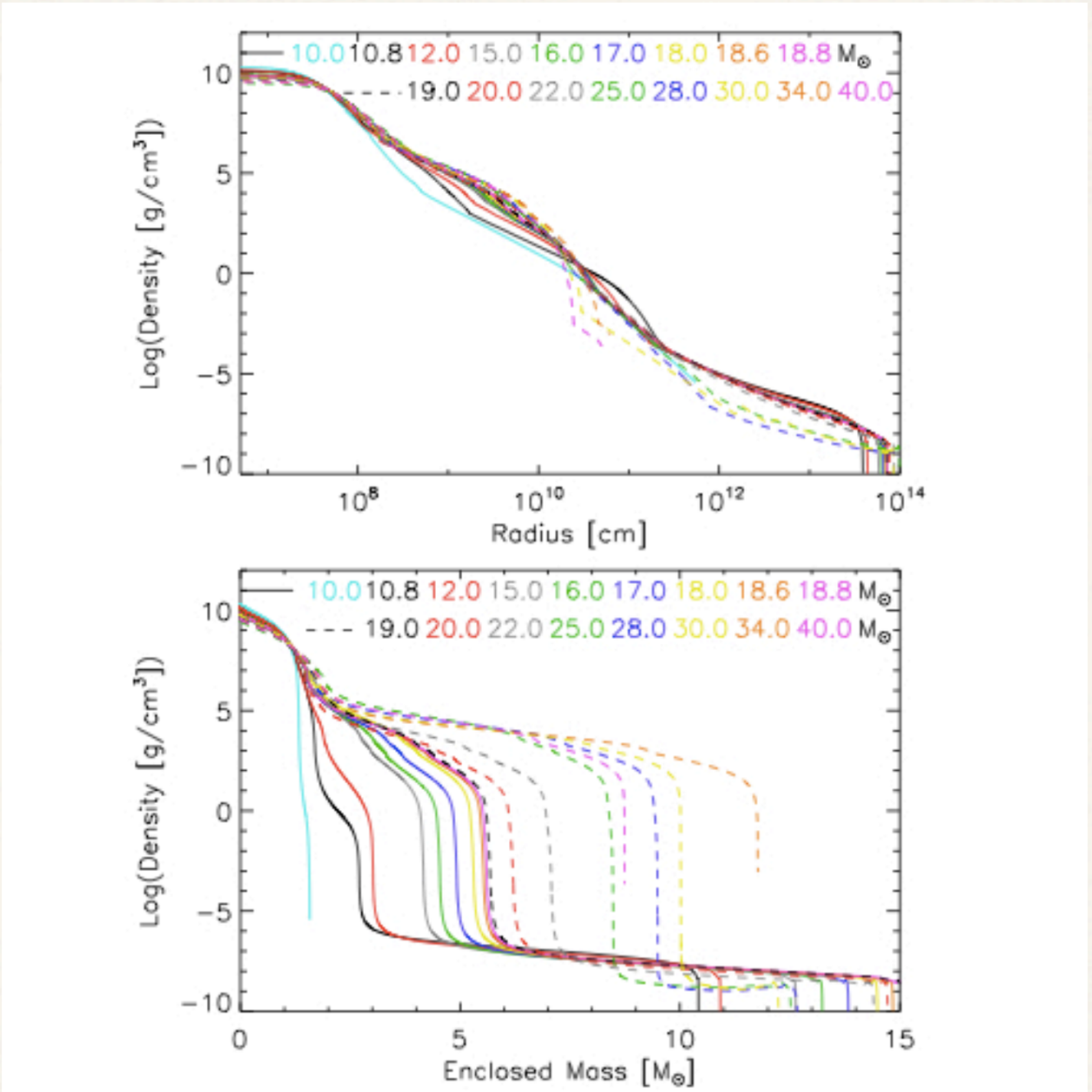

FIG. 2.— Density profiles vs. radius (*top*) and vs. enclosed mass (*bottom*) at the onset of core collapse for a selection of models from the considered set of solar-metallicity progenitors with iron cores. Solid lines correspond to ZAMS masses less than 19 $M_\odot$, dashed lines to higher values. Note that the stellar shell structure and also the high-density core ($\rho \gtrsim 10^5$ g cm^{-3}) exhibit considerable variations with the progenitor mass (see also Fig. 4).

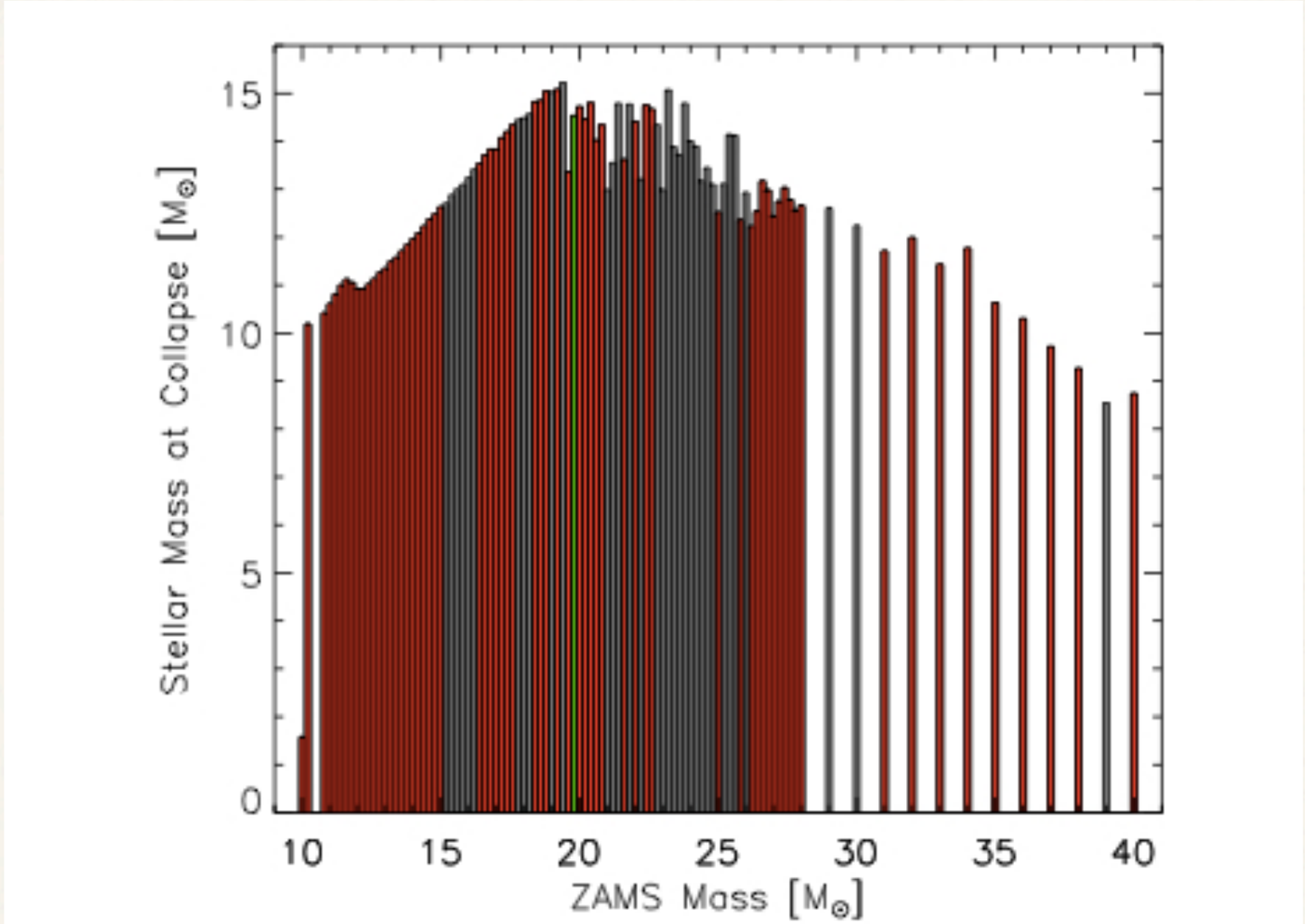

Ugliano, Janka, et al 2012